Upload this completed form to website with submission

ARTICLE INFORMATION	Fill in information in each box below		
Article Type	Research article		
Article Title (within 20 words without abbreviations)	ut SRY-box Transcription Factor 6 and Folliculin-Interactin Protein 1 as Key Regulators of Skeletal Muscle Fib Formation in Chicken		
Running Title (within 10 words)	Analysis of Sox6 and Fnip1 on chicken muscle fiber		
Author	Ji Hoon Park1, Si Eun Kim1, Heesu Jeong1, Ismail Shaleh1,2, Soo Hyun Kim1, Mawar Subangkit3, Tae Sub Park1,4,*		
ORCID (for more information, please visit	1Graduate School of International Agricultural Technology, Seoul National University, Pyeongchanggun, Gangwon-do 25354, South Korea 2Department of Biology, Faculty of Mathematics and Natural Sciences, IPB University, Bogor 16680, Indonesia 3Department of Veterinary Science, School of Veterinary Medicine and Biomedical Science, IPB University, Bogor 16680, Indonesia 4Institute of Green-Bio Science and Technology, Seoul National University, Pyeongchang-gun, Gangwon-do 25354, South Korea Ji Hoon Park (https://orcid.org/0009-0005-3193-0221)		
https://orcid.org)	Si Eun Kim (https://orcid.org/0000-0001-7600-9587) Heesu Jeong (https://orcid.org/0009-0007-5458-6886) Ismail Shaleh (https://orcid.org/0000-0002-7619-9971) Soo Hyun Kim (https://orcid.org/0009-0003-1403-0825) Mawar Subangkit (https://orcid.org/0000-0002-9098-0094) Tae Sub Park (https://orcid.org/0000-0002-0372-5467)		
Competing interests	No potential conflict of interest relevant to this article was reported.		
Funding sources State funding sources (grants, funding sources, equipment, and supplies). Include name and number of grant if available.	This work was supported by the National Research Foundation of Korea (NRF) grant funded by the Korea government (Ministry of Science and ICT) (RS-2025-00556323).		
Acknowledgements	Ismail Shaleh was supported by Korea International Cooperation Agency (KOICA).		
Availability of data and material	Upon reasonable request, the datasets of this study can be available from the corresponding author.		
Authors' contributions Please specify the authors' role using this form.	Conceptualization: Subangkit M, Park TS. Formal analysis: Park JH, Kim SE. Jeong H, Shaleh I, Kim SH. Methodology: Park JH, Kim SE. Jeong H, Shaleh I, Kim SH. Investigation: Park JH, Subangkit M, Park TS. Writing - original draft: Park JH. Writing - review & editing: Park JH, Kim SE, Jeong H, Shaleh I, Kim SH, Subangkit M, Park TS		
Ethics approval and consent to participate	This article does not require IRB/IACUC approval because there are no human and animal participants.		

CORRESPONDING AUTHOR CONTACT INFORMATION

For the corresponding author (responsible for correspondence, proofreading, and reprints)	Fill in information in each box below
First name, middle initial, last name	Tae Sub Park
Email address – this is where your proofs will be sent	taesubpark@snu.ac.kr
Secondary Email address	
Address	Correspondence: Graduate School of International Agricultural Technology and Institute of Green-Bio Science and Technology, Seoul National University, Pyeongchang-gun, Gangwon-do 25354, South Korea
Cell phone number	+82 01 4931 6339
Office phone number	+82 33 339 5721
Fax number	

6 Abstract

SRY-box transcription factor 6 (Sox6) and folliculin-interacting protein 1 (Fnip1) play essential roles in muscle fiber specification during muscle development. However, their involvement in chicken muscle development remains largely unexplored. In this study, CRISPR-Cas9 was used to knock out (KO) Sox6 and Fnip1 in a chicken myoblast cell line (pCM cells). The functional significance and regulatory mechanisms of these genes were then examined during cell proliferation and muscle fiber differentiation. The loss of Sox6 and Fnip1 led to increased expression of Type 1 muscle-specific genes, including myosin light chain 2 (MYL2), myosin heavy chains (MYH1B, MYH1E, and MYH7B), and ATPase sarcoplasmic/endoplasmic reticulum Ca²+ transporting 2 (ATP2A2). In KO pCM cells, the expression of muscle Type 2-specific genes, including MYL1 and Troponin C (TnnC2), was significantly reduced. Moreover, mitochondrial abundance increased following gene deletion. Simultaneously, genes associated with the tricarboxylic acid (TCA) cycle and oxidative phosphorylation exhibited substantially elevated expression in KO pCM cells. Notably, the loss of Sox6 and Fnip1 not only suppressed cell proliferation but also impaired muscle fiber differentiation. Overall, these findings indicate that Sox6 and Fnip1 play a crucial role in regulating muscle fiber specification and differentiation in chickens.

Keywords: chicken, muscle, specification, differentiation, Sox6, Fnip1

Introduction

Skeletal muscle consists of connective tissues and fascicles, which are composed of numerous muscle fibers [1,2]. These muscle fibers are classified into distinct types, each with unique characteristics and structures, enabling an efficient response to physical activity and exercise [1,2]. Based on the analysis of specific enzymes and proteins, muscle fibers are categorized into Type 1 (slow-twitch) and Type 2 (fast-twitch) fibers [3-5]. This classification primarily relies on the examination of myofibrillar adenosine triphosphatase (mATPase) and succinate dehydrogenase (SDH) activity within myosin heavy chain (MHC) [6-8]. Type 1 muscle fibers appear red due to their high content of mitochondria, blood vessels, and myoglobin, which facilitate oxygen delivery and ATP production through the tricarboxylic acid (TCA) cycle and oxidative phosphorylation (OXPHOS) in numerous mitochondria at a relatively slow rate [9,10]. In contrast, Type 2 muscle fibers contain fewer mitochondria, blood vessels, and myoglobin, giving them a white appearance, and generate ATP more rapidly via glycolysis [11,12].

Understanding the regulatory mechanisms of skeletal muscle development has practical applications in the poultry industry [13]. However, research on muscle fiber specification in chickens remains limited. Therefore, we selected candidate genes through comparative analyses with mammalian systems and examined their roles in myogenic differentiation using chick myoblasts because studies on myogenic specification-related genes in chickens are extremely limited. Sox6 and Fnip1 were prioritized for functional validation, as no prior reports have described their involvement in avian myogenesis. This study provides the first functional characterization of Sox6 and Fnip1 during chicken muscle differentiation. In our previous study, we established an immortalized chicken myoblast cell line capable of differentiating into muscle myotubes under specific conditions [14]. We explored the biofunctional roles of SRY-box transcription factor 6 (Sox6) and folliculin-interacting protein 1 (Fnip1), which have been identified as key regulators of muscle fiber specification and differentiation in mammals [15, 16]. In mammalian skeletal muscle, Sox6 functions as a transcriptional repressor of slow-twitch Type 1 myofiber genes, thereby promoting fast-twitch Type 2 myofiber specification. Sox6-knockout mice exhibit enhanced slow-twitch fiber composition, increased mitochondrial content, elevated oxidative metabolism, and improved fatigue resistance, indicating that Sox6 loss-of-function shifts skeletal muscle toward an oxidative phenotype [16]. Fnip1 acts as a negative regulator of AMPK signaling through its interaction with folliculin (FLCN), and Fnip1 deletion relieves AMPK inhibition, resulting in AMPK hyperactivation and downstream PGC-1α-mediated mitochondrial

biogenesis. The Fnip1-deficiency-induced metabolic adaptation promotes slow-twitch oxidative fiber differentiation and enhances fatigue resistance. The conserved roles of Sox6 and Fnip1 in regulating myofiber type specification and oxidative metabolism have been consistently demonstrated across mammalian species including mice and humans [17]. Sox6 is a member of the SoxD subfamily within the Sox gene family and functions as a transcription factor containing a high mobility group (HMG) box DNA-binding domain. This domain enables Sox6 to regulate gene expression by directly binding to specific DNA elements, while its coiled-coil domains facilitate interactions with other transcriptional proteins and microRNAs (miRNAs) [18-20]. Sox6 specifically binds to the 'AACAAT' sequences within slow fiber-specific genes (Myl2, Myl3, Myh1, Myh7, and ATP2a2), repressing their transcription [16]. Fnip1, on the other hand, forms a complex with Fnip2 and Folliculin (Fnip1/Fnip2/Folliculin) through its Longin domain at the N-terminus and DENN domain at the C-terminus [21]. This complex interacts with the mechanistic target of rapamycin complex 1 (mTORC1), which is activated in nutrient-rich conditions [21]. Conversely, AMP-activated protein kinase (AMPK) becomes active under energy-deficient conditions [21]. AMPK activation leads to the phosphorylation of threonine-177 and serine-538 on peroxisome proliferator-activated receptor-γ coactivator-1α (PGC-1α), which then interacts with multiple genes to initiate mitochondrial biogenesis [22-27].

Oxidative-type muscle fibers (Type 1 and Type 2A), characterized by smaller myofiber diameter, higher fiber density expressing red color, enhanced tenderness, improved water-holding capacity, and elevated flavor intensity derived from higher phospholipid content [13]. Biochemically, these fibers maintain elevated glycogen stores and lower ATP degradation rates, resulting in attenuated post-mortem glycolysis and stabilized pH values, thereby mitigating the incidence of PSE (pale, soft, and exudative) meat defects [13]. These traits lead display superior meat quality traits. Conversely, glycolytic-type fibers (Type 2B), characterized by larger fiber diameter and reduced oxidative capacity, exhibit rapid glycolysis with accelerated pH decline post-slaughter, increased shear force values, reduced tenderness, and compromised color stability [13].

In mammals, studies have demonstrated that the specific knockout of Sox6 and Fnip1 leads to a shift from Type 2 to Type 1 muscle fibers. However, research on muscle fiber specification in chickens remains limited. To bridge this knowledge gap, the present study employs the clustered regularly interspaced short palindromic repeats (CRISPR)-Cas9 system to knock out Sox6 and Fnip1 in pCM cells, an immortalized chicken myoblast cell line.

Materials and Methods

pCM Cell Culture and Myotube Differentiation

pCM cells, isolated from the pectoralis major of a 10-day-old chicken embryo, were cultured at 37°C in a 5% CO₂ atmosphere with 60-70% relative humidity [14,28]. The cells were maintained in DMEM High Glucose medium supplemented with 10% fetal bovine serum (FBS) and $1\times$ antibiotic-antimycotic. Subculturing was performed when the cells reached 80% confluency. To induce myotube differentiation, cells were grown to 80% confluency, then washed twice with Dulbecco's Phosphate-Buffered Saline (DPBS; Gibco BRL, Grand Island, NY). The culture medium was then replaced with DMEM High Glucose containing 2% FBS and $1\times$ antibiotic-antimycotic. This differentiation process was continued for seven days to promote myotube formation. Quantitative morphological analysis was performed using ImageJ software. For each experimental group (WT, Sox6 KO, and Fnip1 KO), a minimum of 30 cells from at least 3 independent fields of view in each of 3 biological replicates (total $n \ge 90$ cells per group) were manually traced and analyzed. Cell length was defined as the longest axis from end to end of the cell body. Cell width was measured as the maximum perpendicular distance perpendicular to the length axis. Cell area was calculated by tracing the entire cell boundary using ImageJ's freehand drawing tool, and the software automatically computed the enclosed area in square micrometers (μ m²). All measurements were calibrated using the embedded scale bar, and values were converted from pixels to micrometers.

Construction of Sox6 gRNA and Fnip1 gRNA Expression Vector

The pUC-Amp vector was utilized to generate guide RNAs (gRNAs) targeting the sex-determining region (SRY)-box 6 (Sox6; NCBI Gene ID: 423068) and folliculin-interacting protein 1 (Fnip1; NCBI Gene ID: 427642), both of which function as transcription factors in pCM chicken myoblast cells. A gRNA for Sox6 was designed to target exon 1 using the sequence: 5'-GCA TCA CGA GAC AAG GAA GA-3'. However, due to the absence of a suitable protospacer adjacent motif (PAM) sequence in exon 1 of Fnip1, a target locus (5'-GGA CTG TGA GAG AAG AGG A-3') was selected in exon 2, based on the PAM sequence (CGG). The gRNAs were transcribed under the control of the U6 promoter and terminated by the U6 5'-TTTTTTT-3' terminator sequence. The complete

gRNA sequences were then inserted into the lacZ sequence at the multiple cloning sites (MCS) within the pUC-Amp vector. The high-fidelity variant Cas9 (HF-Cas9) protein was obtained as the CMV-CAS9-2A-GFP plasmid (Sigma-Aldrich, St. Louis, MO) (Suppl. Fig. 1).

Cell Transfection

To generate Sox6 knockout (KO) cells and Fnip1 KO cells, the gRNA vectors were co-transfected with Cas9 vectors using Lipofectamine 3000 (Invitrogen, Waltham, MA) according to the manufacturer's protocol. When the cells reached 80% confluency in 6-well plates, they were washed twice with Dulbecco's Phosphate-Buffered Saline (DPBS) and the media was replaced with 10% fetal bovine serum (FBS) without antibiotic-antimycotic. In total, 7.5 μ L of Lipofectamine reagent, 2 μ g of gRNA vector, 2 μ g of Cas9 expression vector, and 10 μ L of p3000 reagent were mixed in 500 μ L of Opti-MEM (Invitrogen) and added to each well. After a 5-hour incubation, the cells were washed three times with DPBS, and fresh media containing 10% FBS and antibiotic-antimycotic was added. The following day, fluorescence-activated cell sorting (FACS) was performed to isolate GFP-expressing cells.

T-Vector Cloning to Obtain Knock-Out Sequence

Genomic PCR was performed to analyze the sequence. The PCR conditions were as follows: an initial denaturation at 95°C for 3 minutes, followed by 40 cycles of denaturation at 95°C for 30 seconds, annealing at 60°C for 30 seconds, and extension at 72°C for 30 seconds. A final extension step was carried out at 72°C for 5 minutes. The PCR amplicons were then cloned into the pGEM®-T Easy Vector System kit (Promega, Madison, WI) for subsequent genotype sequencing.

Quantitative RT-PCR Analysis

Total RNA was isolated from each cell line using guanidine acid-phenol extraction with Trizol reagent (Invitrogen). The RNA quality and concentration were assessed using a NanoDrop 2000 spectrophotometer

(Thermo Fisher Scientific, Waltham, MA). For cDNA synthesis, 1 μg of total RNA was reverse transcribed using the SuperScriptTM First-Strand Synthesis System for quantitative reverse transcription polymerase chain reaction (qRT-PCR; Invitrogen). Each 25 μL RT-PCR reaction mixture contained 2.5 μL of 10X eTaq reaction buffer (Solgent, Daejeon, Korea), 2 μL of dNTP mixture (Takara, Tokyo, Japan), 10 pmol of forward and reverse primers, 0.2 μL of eTaq (Solgent), 1 μL of cDNA template, and 17.3 μL of ddH₂O. The PCR conditions were as follows: initial denaturation at 95°C for 3 minutes, followed by 40 cycles of 95°C for 30 seconds, 55-60°C (depending on the primers) for 30 seconds, and 72°C for 30 seconds. The reaction was completed with a final extension at 72°C for 5 minutes. The PCR products were then analyzed by electrophoresis on a 1.5% agarose gel.

After confirming a single band by electrophoresis, qRT-PCR was performed to quantify the transcripts (Supplementary Table 1). Each reaction tube contained 2.5 μ L of 10X eTaq reaction buffer (Solgent), 1 μ L of dNTP mixture (Takara), 10 pmol of forward and reverse primers, 1 μ L of EvaGreen (Biotium, Fremont, CA), 0.2 μ L of eTaq, 16.3 μ L of ddH₂O, and 2 μ L of cDNA template. The qRT-PCR conditions were as follows: an initial denaturation at 95°C for 5 minutes, followed by 40 cycles of denaturation at 95°C for 30 seconds, annealing at a temperature specific to the primers (55-60°C) for 30 seconds, and extension at 72°C for 30 seconds. The results were normalized to the expression of β -actin (ACTB) and quantified using the $2^{-\Delta\Delta CT}$ method. All qRT-PCR experiments were performed in quadruplicate.

Protein Extraction and Western Blotting

Cells were lysed with radioimmunoprecipitation assay (RIPA) buffer. Protein concentration was determined using bovine serum albumin (BSA) and a protein assay dye (Bio-Rad, Hercules, CA). The protein samples were then heated at 100°C for 10 minutes, mixed with 6x Laemmli SDS sample buffer (Thermo Scientific). Proteins were separated on a 10% polyacrylamide gel and transferred to a 0.2 μm nitrocellulose membrane (Bio-Rad). The membrane was blocked with skimmed milk for 2 hours, and primary antibodies were incubated overnight at 4°C. The primary antibodies used were β-actin (Santa Cruz Biotechnology, Dallas, TX, cat#Sc-47778), anti-Pax7 (R&D Systems, Minneapolis, MN, cat#MAB1675), and anti-p53 (St. John's Lab, London, UK, cat#STJ140114). Horseradish peroxidase (HRP)-conjugated anti-mouse IgG (Bio-Rad, cat#170-6516) and HRP anti-goat IgG (Bio-Rad, cat#172-1034) were used as secondary antibodies (Supplementary Table 2). Protein bands were detected

using ECL substrate (Bio-Rad) and visualized with a ChemiDocTM XRS+ imaging system (Bio-Rad).

156

157

158

159

160

161

162

163

164

165

166

167

168

169

170

171

172

173

174

175

176

177

155

Cell Proliferation Analysis

Cell proliferation was analyzed using two different methods: a hemocytometer counting method and a 5bromo-2'-deoxyuridine (BrdU) incorporation assay. For the hemocytometer method, cells were seeded into 12well culture plates at an initial density of 0.5×10^4 cells per well in complete culture medium. Cells were maintained at 37°C in a humidified atmosphere containing 5% CO₂. At designated time points (Day 0, 2, 4, and 6), cells were detached using 0.05% trypsin-EDTA for 5 minutes at 37°C. Cell viability was determined by trypan blue (0.4%) exclusion, with only viable (unstained) cells counted using a hemocytometer. For each sample, cell counts were performed in duplicate from 4 wells per time point. Cell counts were calculated as the mean of 4 wells, and experiments were performed in triplicate (n=3 independent experiments, total n=12 wells per time point per group). Growth curves were generated by plotting total cell numbers against time. For the BrdU cell proliferation assay, BrdU cell proliferation assay was conducted using BD PharmingenTM BrdU Flow Kits (Becton, Dickinson and Company, Franklin Lakes, NJ). The cells were seeded at a density of 0.2×106 exceed in 6-well plates two days before BrdU labeling. After two days, 10 µM BrdU was added directly to the cell culture medium. Following a two-hour incubation at 37°C, the cells were detached using Trypsin-EDTA and permeabilized using Cytofix/Cytoperm Buffer and Cytoperm Permeabilization Buffer Plus. Subsequently, the samples were incubated at 37°C for one hour with 300 µg/ml DNase to expose the BrdU epitope for antibody recognition, after which they were stained for total DNA level using 7-amino-actinomycin D (7-AAD). Flow cytometry analysis was performed on a BD FACSAriaTM. Cell cycle phases were defined as follows: G0/G1 phase (2n DNA content, BrdU-negative), S phase (intermediate DNA content, BrdU-positive), and G2/M phase (4n DNA content, BrdU-negative). Apoptotic cells were identified as sub-G1 population (DNA content < 2n). Data from a minimum of 10,000 events per sample were acquired. Results represent mean \pm standard deviation from three independent experiments.

178

179

180

Mitochondrial DNA Analyses

After mitochondrial DNA extraction, the relative abundance of mitochondrial DNA was quantified by qPCR

using primers specific to each DNA type (Supplementary Table 3) [29,30]. To determine the mitochondrial DNA content, the following equation was used:

 $2 \times 2^{\Delta CT}$ where $\Delta CT = (nucDNA CT-mtDNA CT)$

Mitochondria Staining

Cells were washed three times with DPBS for staining. The cells were then incubated with 200 nM MitoTracker® Red CMXRos (Cell Signaling, Danvers, MA) in FluoroBriteTM DMEM (Gibco) containing 10% FBS at 37°C for 20 minutes. Afterward, the cells were washed three times with DPBS, and cold methanol was added. The cells were incubated at -20°C for 15 minutes. The stained cells were measured on a total of 20 cells per each group of three biological replicates (6-7 cells per well from 3 independent wells) using CytationTM imaging Readers (BioTek, Winooski, VT). Using CytationTM, the area corresponding to each individual cell was automatically delineated, and data were quantified based on the median intensity within each defined area.

Statistical Analysis

All quantitative data were analyzed using one-way ANOVA followed by Dunnett's multiple comparison test to compare each knockout group against the WT control. Statistical significance was denoted as follows: *, **, **** indicate p < 0.05, p < 0.01, p < 0.0005, and p < 0.0001, respectively. All statistical analyses were performed using GraphPad Prism 8.0.1 software. Data are presented as mean \pm standard deviation (SD) from a minimum of three independent experiments.

200 Results

Schematic Diagram of Knockout Target Design and Mutant Genotype

To investigate the effects of Sox6 and Fnip1 on chicken muscle cells, we performed CRISPR-Cas9-mediated knockout (KO) of each gene in the pCM cell line, a chicken myoblast isolated from the pectoralis major of a 10-day-old embryo (14,28). After knockout, single-cell-derived sublines with frameshift mutations were identified and selected. Specifically, Sox6 KO#2 and Fnip1 KO#3 were obtained, exhibiting frameshift mutations of a 4 nt/16 nt deletion and a 5 nt deletion/1 nt insertion, respectively (Fig. 1). These frameshift mutations resulted in the production of dysfunctional proteins (Fig. 1).

Morphological Characterization and Analysis of Cell Growth Curve in WT Cells, Sox6 KO, and Fnip1 KO Cells

After identifying the single-cell-derived KO sublines, morphological differences between wild-type (WT) and Sox6 or Fnip1 KO sublines were compared (Fig. 2A). The cell length of Sox6 KO cells was significantly reduced compared to WT cells, while no significant difference was observed in Fnip1 KO cells (Fig. 2B). In contrast, the width of Sox6 KO cells was significantly increased compared to WT cells, with no significant change in Fnip1 KO cells. Interestingly, both KO cell types exhibited a significant increase in cell area. These changes in length and width contributed to a rounded phenotype in Sox6 KO cells (Fig. 2A). Regarding cell proliferation, both Sox6 and Fnip1 KO cells displayed a significant reduction in proliferation compared to WT cells (Fig. 2C), with Fnip1 KO cells exhibiting the lowest proliferation rate (Fig. 2C).

Analysis of Sox6 or Fnip1 on Cell Proliferation

To investigate the functional effects of Sox6 and Fnip1 on cell proliferation, we analyzed cell cycle gene expression patterns using qRT-PCR and Western blotting. The expression of cyclin D1 (CCND1), which forms the CCND1-CDK4 complex essential for regulating the G1/S transition, was significantly reduced in both Sox6 KO and Fnip1 KO cells (Fig. 3A). Additionally, proliferating cell nuclear antigen (PCNA), a cofactor for DNA

polymerase, was markedly decreased in both Sox6 KO and Fnip1 KO cells (Fig. 3A). Insulin-like growth factor 1 receptor (IGF1R), which plays a crucial role in cell growth, was also significantly downregulated in both KO cells (Fig. 3A). Next, we examined gene expression patterns related to the G2/M transition. The expression levels of Cyclin B1 (CCNB1) and Cyclin-Dependent Kinase 1 (CDK1), key components of the CCNB1-CDK1 complex that regulate G2/M progression, were reduced in both Sox6 KO and Fnip1 KO cells (Fig. 3B). Furthermore, a significant decrease in the expression of Aurora Kinase B (AURKB) and Polo-like Kinase 1 (PLK1), which are involved in spindle formation and attachment, was observed (Fig. 3B). Finally, Western blot analysis was performed to assess p53, a master regulator of tumor suppression and cell cycle control. The results demonstrated significantly elevated p53 protein expression in both Sox6 KO and Fnip1 KO cells (p < 0.0001) and 1.5-fold in Fnip1 KO cells (p < 0.001). p53 acts as a cellular stress sensor that induces cell cycle arrest by activating the CDK inhibitor p21/WAF1, which prevents cyclin-CDK complex activity and blocks G1/S phase progression. The correlation between elevated p53 levels and reduced cell proliferation in both knockout cells, suggests that p53-dependent cell cycle checkpoints play a critical role in mediating the growth suppression.

In the subsequent experiment, cell cycle analysis was conducted using the 5-bromo-2'-deoxyuridine (BrdU) incorporation assay (Fig. 4A). The results revealed a significant suppression of the S phase in Sox6 KO (12.1 \pm 0.4%) and Fnip1 KO cells (3.5 \pm 0.2%) compared to WT cells (25.9 \pm 0.2%) (Fig. 4B). Moreover, the proportion of cells arrested in the G2/M phase was notably higher in Sox6 KO (15.8 \pm 0.1%) and Fnip1 KO cells (25.0 \pm 1.0%) compared to WT cells (5.0 \pm 0.1%) (Fig. 4B). These findings suggest that Sox6 and Fnip1 play a role in regulating the cell cycle pathway and influencing proliferation in chicken myoblast cells.

Characterization of Sox6 KO and Fnip1 KO cells in the undifferentiated state

We analyzed the gene expression patterns associated with muscle fiber types in Sox6 KO and Fnip1 KO cells. The expression of paired box 7 (Pax7), a key myoblast marker in the undifferentiated stage, and MyoD, a myogenic regulatory factor (MRF), was significantly downregulated in both Sox6 KO and Fnip1 KO cells (Fig. 5A). Additionally, Western blotting confirmed the reduced expression of Pax7 in Sox6 KO and Fnip1 KO cells compared to WT cells (Fig. 5B). Next, we examined the expression of muscle fiber-specific genes, including

myosin light chain 2 (MYL2) and naked cuticle homolog 1 (NKD1), which are highly expressed in Type 1 muscle fibers. The expression of Type 1 muscle fiber-specific genes was significantly increased in Sox6 KO and Fnip1 KO cells, except for MYL2 in Fnip1 KO cells (Fig. 5C). Type 2 muscle fiber-specific genes, including MYL1, a fast skeletal muscle-specific myofibrillar protein gene, troponin C2 (TnnC2), a cardiac troponin subunit gene, and ryanodine receptor 1-like (RYR1), were significantly downregulated in Sox6 KO and Fnip1 KO cells (Fig. 5D).

Knockout of Sox6 and Fnip1 enhances mitochondrial content in skeletal muscle cells

Type 1 muscle fibers contain a higher abundance of mitochondria compared to Type 2 muscle fibers. Therefore, we assessed mitochondrial content in WT and KO cells using the MitoTracker reagent (Fig. 6A). The red fluorescence intensities of the MitoTracker reagent were measured and compared between WT and KO cells, revealing significantly higher intensities in Sox6 KO and Fnip1 KO cells relative to WT cells (Fig. 6B). These findings were consistent with qRT-PCR data showing increased mitochondrial DNA content and upregulation of mitochondrial biogenesis genes, including peroxisome proliferator-activated receptor gamma coactivator 1-alpha (PGC-1α), as well as its downstream regulatory genes nuclear respiratory factor 1 (NRF1) and mitochondrial transcription factor A (TFAM) (Fig. 6C). Overall, these results suggest that the absence of Sox6 and Fnip1 promotes mitochondrial biogenesis in chicken myoblast cells.

Knockout of Sox6 and Fnip1 inhibits myocyte differentiation

pCM cells, as myoblasts, have the potential to differentiate into myocytes and myotubes under specific conditions (Suppl Fig. 2A). Interestingly, the expression levels of Sox6 and Fnip1 in WT cells gradually and significantly increased during myocyte differentiation, from day 0 (undifferentiated) to day 7 (Suppl Fig. 2B). In contrast, Sox6 KO and Fnip1 KO cells exhibited a dramatic reduction in myotube formation compared to WT cells, with significantly decreased myotube differentiation percentages and areas (Fig. 7). Additionally, the nuclear fusion rates within each myotube were significantly lower in Sox6 KO and Fnip1 KO cells after 7 days of differentiation (Fig. 7C). qRT-PCR data revealed similar gene expression patterns in Sox6 KO and Fnip1 KO cells after myotube differentiation (Fig. 8). The expression levels of Pax7 and MyoD, which are muscle-specific genes

in the undifferentiated state, as well as myogenin and desmin, which are key myogenic genes, were downregulated in both Sox6 KO and Fnip1 KO cells (Fig. 8A). These findings suggest that Sox6 and Fnip1 play a crucial role in regulating myogenic pathways in chicken muscle development.

Effects of Sox6 and Fnip1 on muscle fiber specification in chicken

We investigated the effects of Sox6 and Fnip1 on muscle fiber specification during myocyte differentiation. qRT-PCR analysis revealed a significant increase in Type 1 muscle fiber-specific gene expression in both Sox6 KO and Fnip1 KO cells after myotube differentiation (Fig. 8B). The expression levels of myosin heavy chain 7B (MYH7B), myosin heavy chain 1B (MYH1B), and myosin heavy chain 1E (MYH1E), which encode slow myofibrillar proteins, were markedly elevated in Sox6 KO and Fnip1 KO cells. Additionally, myosin light chain 2 (MYL2) and ATPase sarcoplasmic/endoplasmic reticulum Ca²⁺ transporting 2 (ATP2A2), which are highly expressed in Type 1 muscle fibers, were also significantly upregulated (Fig. 8B). These findings suggest that Sox6 and Fnip1 are also involved in muscle fiber specification, particularly in the regulation of slow-twitch muscle fiber formation.

The absence of Sox6 and Fnip1 enhances glucose metabolism activity.

Type 1 muscle fibers rely more heavily on mitochondria than Type 2 muscle fibers, enabling efficient ATP production through the TCA cycle and OXPHOS. Given our previous findings of increased mitochondrial volume in Sox6 KO and Fnip1 KO cells, we conducted a comparative gene expression analysis of glucose metabolism and mitochondrial regulatory pathways between WT and mutant pCM sublines (Sox6 and Fnip1 KO) following myotube differentiation. Notably, the expression of v-myc avian myelocytomatosis viral oncogene homolog (C-MYC), which interacts with both Sox6 and Fnip1, was upregulated. Increased C-MYC expression is known to directly activate the transcription of nearly all related genes. To investigate its impact, we examined the expression levels of glucose transporter type 1 (GLUT1) and glucose transporter type 3 (GLUT3), which interact with C-MYC. The results showed that GLUT1 and GLUT3 expression was elevated in Sox6 KO and Fnip1 KO cells compared to WT cells (Fig. 9A). Since higher GLUT expression facilitates increased glucose uptake, the

expression of enzymes involved in glucose metabolism was also upregulated. The expression levels of phosphoglucomutase 1 (PGM1) and phosphoglucomutase 2 (PGM2) genes encoding phosphoglucomutase which is an enzyme responsible for converting glucose 1-phosphate to glucose 6-phosphate, were significantly elevated in Sox6 KO and Fnip1 KO cells compared to WT cells. Furthermore, hexokinase 1 (HK1), which encodes hexokinase catalyzing the conversion of glucose to glucose 6-phosphate, was notably upregulated in Sox6 KO and Fnip1 KO cells relative to WT cells. Interestingly, we also observed increased expression of glucose-6-phosphate isomerase (GPI), the enzyme that interconverts glucose 6-phosphate and fructose 6-phosphate, in both Sox6 KO and Fnip1 KO cells. Additionally, lactate dehydrogenase A (LDHA), which facilitates the conversion of pyruvate to lactate, was significantly overexpressed in Sox6 KO and Fnip1 KO cells compared to WT (Fig. 9B).

It is well established that pyruvate generated in this process must be converted into acetyl-CoA to successfully enter the TCA cycle. As a result, acetyl-CoA conversion is more prevalent in muscle Type 1 fibers than in muscle Type 2 fibers. To investigate this, we examined the expression levels of pyruvate dehydrogenase E1 subunit beta (PDHB), which encodes the pyruvate dehydrogenase complex, as well as dihydrolipoamide S-acetyltransferase (DLAT) and dihydrolipoamide dehydrogenase (DLD). The results revealed that PDHB, DLAT, and DLD expression was elevated in Sox6 KO and Fnip1 KO cells compared to WT cells (Fig. 9C). Additionally, we analyzed gene expression related to the mitochondrial electron transport system. This included succinate dehydrogenase complex flavoprotein subunit A (SDHA), a key component of respiratory chain complex II; cytochrome C (CYCS), which facilitates electron transfer between respiratory chain complexes III and IV; cytochrome C oxidase subunit 5A (COX5A), involved in complex IV; and ATP synthase F1 subunit alpha (ATP5A1), which encodes part of the ATP synthase complex. The expression levels of these genes were significantly increased in Sox6 KO and Fnip1 KO cells relative to WT cells (Fig. 9D). These findings suggest that the knockout of Sox6 and Fnip1 enhances glucose metabolism activity.

326 Discussion

This study employs the CRISPR/Cas9 system to knock out Sox6 and Fnip1 in pCM, a myoblast cell line derived from chicken pectoral muscle. The goal was to investigate the effects of these genes on chicken muscle cells, not only regarding muscle fiber specification but also in relation to cell proliferation, differentiation, mitochondrial biogenesis, and glucose metabolism. The key conclusion of this study is that Sox6 and Fnip1 form an essential signaling pathway involved in the specification of skeletal muscle fibers in chickens. These findings align with observations made in the mammalian model, particularly in mice [15, 16], indicating that these two genes have a conserved function across species.

An increase in cell size was observed in Sox6 KO and Fnip1 KO cells compared to WT cells, likely linked to cell cycle arrest. Previous studies have shown that when the cell cycle is arrested due to genetic or environmental factors, cells continue to grow until they reach a specific size [31]. This phenomenon supports the hypothesis that the cell cycle arrest caused by the deletion of Sox6 and Fnip1 contributes to the observed increase in cell size. Additionally, the larger cell size may also be associated with an increase in mitochondrial content. A higher number of mitochondria was observed in Sox6 KO and Fnip1 KO cells, suggesting that these cells may require a larger cytoplasmic space to accommodate the increased mitochondrial population. Therefore, mitochondrial expansion is also a contributing factor to the observed increase in cell size.

Cell cycle arrest plays a crucial role in muscle cell differentiation [32], as it typically facilitates myoblast differentiation. Once myoblasts exit the cell cycle, myogenic regulatory factors such as MyoD and MyoG drive muscle differentiation [33]. However, in this study, despite the inhibition of cell proliferation, the expression of MyoD and MyoG which are key genes involved in myogenic differentiation, was significantly suppressed in Sox6 KO and Fnip1 KO cells compared to WT cells. Similarly, desmin, a marker of terminal myotube differentiation, was also downregulated. During muscle development, MyoD and Sox6 play essential and closely interacting roles. MyoD undergoes histone H4 acetylation and binds to myotubes during muscle differentiation, while Sox6 also binds to myotubes during myogenesis. Notably, the majority (96%) of MyoD and Sox6 binding sites either overlap or are located within 50 base pairs of each other [34]. Furthermore, the E-box motif, identified within Sox6 binding sites, is predominantly linked to genes regulating muscle differentiation. Consequently, in the absence of Sox6, MyoD is unable to bind to these sites, disrupting the precise regulation of muscle-specific gene expression [35].

We observed increased expression of MYH7B, MYH1B, MYL2, ATP2A2, and MYH1E in myocyte-differentiated Sox6 KO cells, consistent with findings from previous researches. Studies on the interaction between Fnip1 and PGC-1α have predominantly reported elevated expression of muscle Type 1 fiber marker MYH7 and enhanced mitochondrial activity [15,35,36]. However, this study presented a unique finding: an increase in the expression of genes associated with slow myofibers. Notably, at the myoblast stage, the deletion of Sox6 and Fnip1 led to increased expression of NKD1. Given that Wnt/β-catenin signaling is known to drive the conversion of slow myofibers into fast myofibers, and NKD1 acts as a potent inhibitor of this pathway [37,38], the elevated NKD1 expression following Sox6 and Fnip1 deletion suggests that it may contribute to the maintenance of slow myofiber characteristics by suppressing Wnt/β-catenin signaling.

Fnip1 has been shown to interact with AMPK, folliculin (FLCN), Fnip2, and HSP90. In a study on renal cancer cells, FLCN deletion led to increased PGC-1 α expression, enhancing mitochondrial function and oxidative metabolism [23,37]. Similarly, in Fnip1-deficient skeletal muscle, elevated PGC-1 α / β expression and upregulation of mitochondrial components (ATP5g, Cox5a, Cycs, Pdk4, Ndufs8, Ucp3) involved in the electron transport chain (ETC) and TCA cycle [15,23]. Likewise, the deletion of either Fnip1 or FLCN alone has been found to increase PGC-1 α expression. This occurs because Fnip1 and FLCN regulate the phosphorylation of PGC-1 α at threonine-177 [23]. In line with these findings, we speculate that the deletion of Fnip1 in this study leads to PGC-1 α activation, subsequently promoting mitochondrial biogenesis. Additionally, we observed that the knockout of Sox6 also increased PGC-1 α expression, which aligns with recent studies suggesting a Sirt6-CREB-Sox6 axis. A previous study proposed that Sirtuin 6 (Sirt6) enhances PGC-1 α expression by activating cAMP response element-binding protein (CREB) while inhibiting Sox6 [38]. By directly inhibiting Sox6, which plays a central role in this axis, we found that Sox6 suppression resulted in increased PGC-1 α expression.

Previous research has shown that slow-twitch muscles exhibit low glycolytic enzyme activity, whereas fast-twitch muscles primarily generate ATP via the glycolytic pathway to enable rapid muscle contraction [36]. In this study, Sox6 KO and Fnip1 KO cells displayed several notable changes compared to wild-type (WT) cells. Firstly, the expression of GLUT1 and GLUT3 was elevated, leading to an increase in glycolysis-related enzymes, including HK1, PGM1, PGM2, PGI, and LDHA. Additionally, genes encoding enzymes involved in the conversion of pyruvate to acetyl-CoA (DLD, PDHB, DLAT) and genes associated with the electron transport chain (SDHA, CYCS, COX5A, ATP5A1) were also upregulated. These findings suggest that Sox6 KO and Fnip1

KO cells have undergone a shift from fast-twitch to slow-twitch muscle characteristics. On the other hand, Sox6 directly binds to an upstream region of the c-Myc sequence, inhibiting its expression [37]. Therefore, the deletion of Sox6 and Fnip1 may promote c-Myc expression. Sox6 knockout removes the direct repression of c-Myc, while the Fnip1 knockout leads to indirect upregulation of c-Myc through the activation of STAT3 signaling [38]. The elevated expression of c-Myc results in increased GLUT1 expression, which enhances glucose uptake [39]. Studies using D-glucose protectable cytochalasin B binding in adult rodent skeletal muscle fibers have shown that GLUT1 expression is higher in the plasma membrane of red muscle than in white muscle [40]. Similarly, GLUT3 has been reported to exhibit greater expression in human slow-twitch muscle fibers, as identified by NADHtetrazolium reductase staining [41]. Both GLUT1 and GLUT3 contribute to basal glucose uptake. The increased mitochondrial content observed in Sox6 KO and Fnip1 KO cells suggests enhanced oxidative ATP production capacity, which requires a higher basal glucose supply to sustain glucose oxidation. Consequently, we propose that the upregulation of GLUT1 and GLUT3 in Sox6 KO and Fnip1 KO cells is likely driven by elevated c-Myc expression. Thus, the Sox6 KO and Fnip1 KO cells in this study have activated glycolysis through enhanced c-Myc expression. Moreover, myoblast differentiation is inhibited by the upregulation of glucose uptake, which in turn decreases the expression of MyoD and MyoG [42]. These findings may help explain the disruption of differentiation observed in both Sox6 KO and Fnip1 KO cells.

381

382

383

384

385

386

387

388

389

390

391

392

393

394

395

396

397

398

399

400

This study examined the roles of Sox6 and Fnip1 in chicken muscle cells through loss-of-function experiments. The deletion of Sox6 and Fnip1 impairs cell proliferation and differentiation, while simultaneously activating glucose metabolism. Conclusively, these genes are involved in muscle fiber specification in chicken (Fig. 10).

401	Competing interests
402	No potential conflict of interest relevant to this article was reported.
403	
404	Funding sources
405	This work was supported by the National Research Foundation of Korea (NRF) grant funded by the Korea
406	government (Ministry of Science and ICT) (RS-2025-00556323).
407	
408	Acknowledgement
409	Ismail Shaleh was supported by Korea International Cooperation Agency (KOICA).
410	
411	Authors' contributions
412	Conceptualization: Subangkit M, Park TS.
413	Formal analysis: Park JH, Kim SE. Jeong H, Shaleh I, Kim SH.
414	Methodology: Park JH, Kim SE. Jeong H, Shaleh I, Kim SH.
415	Investigation: Park JH, Subangkit M, Park TS.
416	Writing - original draft: Park JH.
417	Writing - review & editing: Park JH, Kim SE, Jeong H, Shaleh I, Kim SH, Subangkit M, Park TS
418	
419	Ethics approval and consent to participate
420	This article does not require IRB/IACUC approval because there are no human and animal participants.
421	
422	Availability of data and material
423	Upon reasonable request, the datasets of this study can be available from the corresponding author.

424 References

- 1. Frontera WR, Ochala J. Skeletal muscle: a brief review of structure and function. Calcif Tissue Int. 2015;
- 426 96:183-95
- 427 2. Scott W, Stevens J, Binder-Macleod SA. Human skeletal muscle fiber type classifications. Phys Ther. 2001;
- 428 81:1810-6
- 3. Edman AC, Lexell J, Sjostrom M, Squire JM. Structural diversity in muscle fibres of chicken breast. Cell Tissue
- 430 Res. 1988; 251:281-9
- 4. Barnard EA, Lyles JM, Pizzey JA. Fibre types in chicken skeletal muscles and their changes in muscular
- 432 dystrophy. J Physiol. 1982; 331:333-54
- 5. Schiaffino S, Reggiani C. Fiber types in mammalian skeletal muscles. Physiol Rev. 2011; 91:1447-1531
- 6. Brooke MH, Kaiser KK. Three "myosin adenosine triphosphatase" systems: the nature of their pH lability and
- sulfhydryl dependence. J Histochem Cytochem. 1970; 18:670-2
- 7. Bandman E, Rosser BW. Evolutionary significance of myosin heavy chain heterogeneity in birds. Microsc Res
- 437 Tech. 2000; 50:473-91
- 8. Bandman E, Matsuda R, Strohman RC. Developmental appearance of myosin heavy and light chain isoforms
- in vivo and in vitro in chicken skeletal muscle. Dev Biol. 1982; 93:508-18
- 9. Jansson E, Sylvén C. Myoglobin concentration in single type I and type II muscle fibres in man. Histochemistry.
- 441 1983; 78:121-4
- 10. Ordway GA, Garry DJ. Myoglobin: an essential hemoprotein in striated muscle. J Exp Biol. 2004; 207:3441-
- 443
- 11. Fernie AR, Carrari F, Sweetlove LJ. Respiratory metabolism: glycolysis, the TCA cycle and mitochondrial
- electron transport. Curr Opin Plant Biol. 2004; 7:254-61
- 446 12. Chandel NS. Glycolysis. Cold Spring Harb Perspect Biol. 2021;13
- 13. Mo M, Zhang Z, Wang X, Shen W, Zhang L, Lin S. Molecular mechanisms underlying the impact of muscle
- fiber types on meat quality in livestock and poultry. Front Vet Sci. 2023; 10:128455.
- 14. Kim SW, Lee JH, Park TS. Functional analysis of SH3 domain containing ring finger 2 during the myogenic
- differentiation of quail myoblast cells. Asian-Australas J Anim Sci. 2017; 30(8):1183-9
- 451 15. Reyes NL, Banks GB, Tsang M, Margineantu D, Gu H, Djukovic D, et al. Fnip1 regulates skeletal muscle
- fiber type specification, fatigue resistance, and susceptibility to muscular dystrophy. Proc Natl Acad Sci USA.
- 453 2015; 112:424-9
- 454 16. Quiat D, Voelker KA, Pei J, Grishin NV, Grange RW, Bassel-Duby R, et al., Concerted regulation of myofiber-
- 455 specific gene expression and muscle performance by the transcriptional repressor Sox6. Proc Natl Acad Sci
- 456 USA 2011; 108:10196-201
- 457 17. Xiao L, Liu J, Sun Z, Yin Y, Mao Y, Xuet D, et al. AMPK-dependent and -independent coordination of
- 458 mitochondrial function and muscle fiber type by FNIP1. PLoS Genet. 2021; 17:e1009488.18. Hagiwara N.
- Sox6, jack of all trades: a versatile regulatory protein in vertebrate development. Dev Dyn. 2011; 240:1311-
- 460 21

- 19. Saleem M, Barturen-Larrea P, Gomez JA. Emerging roles of Sox6 in the renal and cardiovascular system.
- 462 Physiol Rep. 2020; 8:e14604
- 463 20. Kamachi Y, Uchikawa M, Kondoh H. Pairing SOX off: with partners in the regulation of embryonic
- development. Trends Genet. 2000; 16:182-7
- 465 21. Reyes JMJ, Cuesta R, Pause A. Folliculin: A Regulator of Transcription Through AMPK and mTOR Signaling
- 466 Pathways. Front Cell Dev Biol. 2021; 9:667311
- 467 22. Lin J, Wu H, Tarr PT, Zhang C, Wu Z, Boss O, et al. Transcriptional co-activator PGC-1 alpha drives the
- formation of slow-twitch muscle fibres. Nature. 2002; 418:797-801
- 469 23. Jäger S, Handschin C, St-Pierre J, Spiegelman BM. AMP-activated protein kinase (AMPK) action in skeletal
- 470 muscle via direct phosphorylation of PGC-1alpha. Proc Natl Acad Sci USA 2007; 104:12017-22
- 24. Liang H, Ward WF. PGC-1alpha: a key regulator of energy metabolism. Adv Physiol Educ. 2006; 30:145-51
- 472 25. Uchiumi T, Kang D. The role of TFAM-associated proteins in mitochondrial RNA metabolism. Biochim
- 473 Biophys Acta. 2012; 1820:565-70
- 26. Picca A, Lezza AM. Regulation of mitochondrial biogenesis through TFAM-mitochondrial DNA interactions:
- Useful insights from aging and calorie restriction studies. Mitochondrion. 2015; 25:67-75
- 476 27. Quan Y, Xin Y, Tian G, Zhou J, Liu X. Mitochondrial ROS-Modulated mtDNA: A Potential Target for Cardiac
- 477 Aging. Oxid Med Cell Longev. 2020; 9423593
- 478 28. Lee JH, Park JW, Kang KS, Park TS. Forkhead box O3 promotes cell proliferation and inhibits myotube
- differentiation in chicken myoblast cells. Br Poult Sci. 2019; 60:23-30
- 480 29. Leuthner TC, Hartman JH, Ryde IT, Meyer JN. PCR-Based Determination of Mitochondrial DNA Copy
- Number in Multiple Species. Methods Mol Biol. 2021; 2310:91-111
- 482 30. Rooney JP, Ryde IT, Sanders LH, Howlett EH, Colton MD, Colton MD, et al. PCR based determination of
- 483 mitochondrial DNA copy number in multiple species. Methods Mol Biol. 2015; 1241:23-38
- 484 31. Demidenko ZN, Blagosklonny MV. Growth stimulation leads to cellular senescence when the cell cycle is
- 485 blocked. Cell Cycle. 2008; 7:3355-61
- 486 32. Lee J, Hong F, Kwon S, Kim SS, Kim DO, Kang HS, et al. Activation of p38 MAPK induces cell cycle arrest
- 487 via inhibition of Raf/ERK pathway during muscle differentiation. Biochem Biophys Res Commun.2002;
- 488 298:765-71
- 489 33. Fernández AM, Dupont J, Farrar RP, Lee S, Stannard B, Roith DL. Muscle-specific inactivation of the IGF-I
- receptor induces compensatory hyperplasia in skeletal muscle. J Clin Invest. 2002; 109:347-55
- 34. Cao Y, Yao Z, Sarkar D, Lawrence M, Sanchez GJ, Parker MH, et al. Genome-wide MyoD binding in skeletal
- 492 muscle cells: a potential for broad cellular reprogramming. Dev Cell. 2010; 18:662-74
- 493 35. An CI, Dong Y, Hagiwara N. Genome-wide mapping of Sox6 binding sites in skeletal muscle reveals both
- direct and indirect regulation of muscle terminal differentiation by Sox6. BMC Dev Biol. 2011; 11:59
- 495 36. Wang H, Shen Z, Zhou X, Yang S, Yan F, He K, et al. Identification of Differentially Expressed Genes in
- 496 Different Types of Broiler Skeletal Muscle Fibers Using the RNA-seq Technique. Biomed Res Int. 2020;
- 497 9478949

- 498 37. Zhang G, Chen X, Yu C, Cui L, Chen N, Yi G, et al. FNIP1 suppresses colorectal cancer progression through 499 inhibiting STAT3 phosphorylation and nuclear translocation. iScience. 2024; 27:110730
- 38. Wang J, Ding S, Duan Z, Xie Q, Zhang T, Zhang X, et al. Role of p14ARF-HDM2-p53 axis in SOX6-mediated
 tumor suppression. Oncogene. 2016; 35:1692-702
- 39. Osthus RC, Shim H, Kim A, Li Q, Reddy R, Mukherjee M, et al. Deregulation of glucose transporter 1 and glycolytic gene expression by c-Myc. J Biol Chem. 2000; 275:21797-800
- 41. Marette A, Richardson JM, Ramlal T, Balon TW, Vranic M, Pessin JE, et al. Abundance, localization, and
 insulin-induced translocation of glucose transporters in red and white muscle. Am J Physiol. 1992; 263:C443 52
- 507 42. Stuart CA, Wen G, Peng BH, Popov VL, Hudnall SD, Campbell GA. GLUT-3 expression in human skeletal
 508 muscle. Am J Physiol Endocrinol Metab. 2000; 279:E855-6142. Luo W, Ai L, Wang BF, Zhou Y. High
 509 glucose inhibits myogenesis and induces insulin resistance by down-regulating AKT signaling. Biomed
 510 Pharmacother. 2019; 120:109498

Figure Legends

Figure 1. The mutant genotypes of (A) Sox6 and (B) Fnip1 genes generated via CRISPR-Cas9. (A) The Sox6 knockout (KO) pCM subline#2 exhibited 4nt and 16nt deletions. (B) The Fnip1 KO pCM subline#3 carried a 5nt deletion and a 1nt insertion. Both mutant sublines introduced frameshift mutations, resulting in premature stop codons within the open reading frames (asterisks denote stop codons in the boxed sequences). Target sequences are highlighted in yellow, while protospacer-adjacent motif (PAM) sequences are highlighted in green. Deletion or insertion mutations are represented by red lines.

Figure 2. Morphological differences and proliferation rate comparisons between wild-type (WT) and mutant pCM sublines (Sox6 and Fnip1 KO). (A) Morphological variations between WT and mutant pCM sublines (Sox6 and Fnip1 KO, Scale bar = 200 μ m). (B) Comparative analysis of cell length, width, and area among WT, Sox6 KO, and Fnip1 KO pCM cells. Data are presented as mean \pm SD (*, **, **** represent p < 0.05, p < 0.0005, and p < 0.0001, respectively; n = 30). (C) Proliferation rates of WT, Sox6 KO, and Fnip1 KO pCM cells. Growth rates of WT, Sox6 KO, and Fnip1 KO cells are represented by circles (\bullet), rhombuses (\spadesuit), and triangles (\blacktriangle), respectively (* denotes p < 0.05, **** denotes p < 0.0001).

Figure 3. Comparative gene expression analysis of cell cycle regulators in WT and mutant pCM sublines (Sox6 and Fnip1 KO). (A) Quantitative RT-PCR analysis of cell cycle regulatory genes involved in the G1/S transition. (B) Quantitative RT-PCR analysis of genes regulating the G2/M transition. (C) Western blot analysis and relative expression levels of p53 protein in WT and mutant pCM sublines (Sox6 and Fnip1 KO). Data are presented as mean \pm SD (*, ***, ****, ***** denote p < 0.05, p < 0.01, p < 0.0005, and p < 0.0001, respectively; n = 4 for qRT-PCR and n = 3 for Western blot).

536

Figure 4. Cell cycle analysis using BrdU incorporation assay and 7-AAD staining. (A) Flow cytometry was performed to assess the cell cycle after BrdU incorporation and 7-AAD staining. (B) Comparison of cell cycle distribution between WT and mutant pCM sublines (Sox6 and Fnip1 KO). The percentage distribution of cells in

each phase of the cell cycle is shown. Data are presented as mean \pm SD (*** and **** denote p < 0.0005 and p <

0.0001, respectively; n = 3).

542

540

541

543

544

545

546

547

548

549

550

Figure 5. Comparative expression analysis of myogenic and muscle fiber-specific genes in WT and mutant pCM

sublines (Sox6 and Fnip1 KO). (A) qRT-PCR analysis of myogenic genes (Pax7 and MyoD). (B) Western blotting

and relative expression analysis of Pax7 protein in undifferentiated WT and mutant pCM sublines (Sox6 and Fnip1

KO). (C) Comparative expression analysis of muscle fiber-specific genes. MYL2 and NKD1 are markers for type

1 (slow-twitch) muscle fibers, while MYL1, TnnC2, and RYR1 are specific to type 2 (fast-twitch) muscle fibers.

Data are presented as mean \pm SD (*, **, ***, **** indicate p < 0.05, p < 0.01, p < 0.0005, and p < 0.0001,

respectively; n = 4 for qRT-PCRs and n = 3 for Western blotting).

551

552

553

554

555

556

557

Figure 6. Analysis of mitochondrial content and comparative gene expression in WT and mutant pCM sublines

(Sox6 and Fnip1 KO). (A) MitoTracker® staining to assess mitochondrial content in WT, Sox6 KO, and Fnip1

KO pCM cells. (B) Quantification of MitoTracker® intensities and mitochondrial DNA (mtDNA) levels via qPCR,

expressed as the ratio of mitochondrial (D-loop) to nuclear (VIM) DNA in WT and mutant pCM sublines. (C)

Comparative gene expression analysis of mitochondrial biogenesis using qRT-PCR. Data are presented as mean

 \pm SD (*, **, and *** indicate p < 0.05, p < 0.01, and p < 0.0005, respectively; n = 4).

559

Figure 7. Morphological changes in WT and mutant pCM sublines (Sox6 and Fnip1 KO) during myotube differentiation. (A) Morphological changes and (B) DAPI-stained nuclei of WT, Sox6, and Fnip1 KO pCM cells following myotube differentiation. Arrows indicate multinucleated myotubes under differentiation conditions. (C) Comparative analysis of morphological differences post-differentiation. The percentage of the differentiated area was calculated as the ratio of the differentiated area to the total area. The number of fused nuclei was determined by averaging the nuclei count in differentiated myotubes after DAPI staining. The area per myotube represents the average area of differentiated myotubes in WT, Sox6, and Fnip1 KO pCM cells. Data are presented as mean \pm SD (**** indicates p < 0.0001; n = 30).

Figure 8. The comparative expression analysis of myogenic and muscle fiber-specific genes between WT and mutant pCM sublines (Sox6 and Fnip1 KO) following myotube differentiation. (A) qRT-PCR analysis of myogenic genes (pax7 and MyoD) and markers of myotube differentiation (Myogenin and Desmin). (B) Comparative expression analysis of muscle fiber Type 1-specific genes (slow-twitch muscle). All data are presented as mean \pm SD (** p < 0.01, *** p < 0.0005, **** p < 0.0001; n = 4 for qRT-PCRs).

Figure 9. The comparative gene expression analysis of glucose metabolism and mitochondrial regulatory pathways between WT and mutant pCM sublines (Sox6 and Fnip1 KO) following myotube differentiation. qRT-PCR analysis of (A) glucose transporters (c-myc, GLUT1, and GLUT3) and (B) glucose metabolism-related genes (HK1, PGM1, PGM2, GPI, and LDHA). Gene expression analysis of (C) pyruvate dehydrogenase complex genes (PDHB, DALT, and DLD) and (D) electron transport chain genes (SDHA, CYCS, COX5A, and ATP5A1). All data are presented as mean \pm SD (* p < 0.05, ** p < 0.01, *** p < 0.0005, **** p < 0.0001; p = 4).

Figure 10. The regulatory models for muscle fiber specification pathways in chickens. (A) The regulatory networks of Sox6 and Fnip1 in the proliferation and specification of chicken myoblast cells (pCM cells). (B) The regulatory pathway for glucose metabolism and mitochondrial biogenesis during chicken muscle fiber differentiation.

Supplementary Figure 1. The genomic structure of (A) target loci and (B) gRNA expression vectors for knocking out the chicken Sox6 and Fnip1 genes. (A) Exons are highlighted in blue (exon 1 of Sox6 and exon 2 of Fnip1), while the target sequences are in red and the protospacer-adjacent motif (PAM) sequences in green. Primer sequences are underlined. (B) The U6 promoter is shown in blue, with CRISPR RNAs (crRNAs) and transactivating crRNAs (tracrRNAs) represented in red and yellow, respectively. U6 terminators are marked in purple. These fragments were inserted between the EcoR1 and HindIII restriction sites within the multiple cloning site (MCS) of the pUC57-Amp vector.

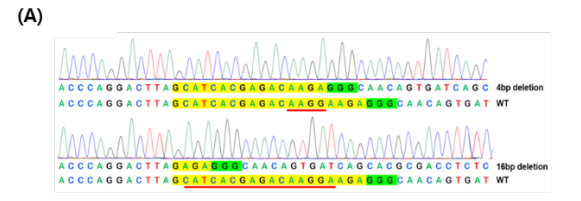
Supplementary Figure 2. Morphological changes and gene expression analysis of wild-type pCM cells during myotube differentiation. (A) Morphological changes observed in pCM cells over four days under differentiation conditions. (B) Expression dynamics of Sox6 and Fnip1 genes during myotube differentiation. Data are presented as mean \pm SD (**, ***, and **** indicate p < 0.01, p < 0.0005, and p < 0.0001, respectively; n = 4).

605 **Figure 1.**

606

607

608





Sox6 wild-type
CAGGACTTAGCATCACGAGACAAGGAAGAGGGCAACAGTGA

Sox6 KO#2: 4nt/16nt del
CAGGACTTAGCATCACGAGACAAG----AGGGCAACAGTGA
CAGGACTTAG-----------AGAGGCAACAGTGA
16nt del

Sox6 wild-type (exon1)
MSSKQATSPFACAADGEETMTQDLASRDKEEGNSDQHATSHLPLHNVMHNKPHSE
ELPTLVTTIQQDAEWDGVISAQHRM

Sox6 KO#2 (4nt del)
MSSKQATSPFACAADGEETMTQDLASRDKRATVISTRPLICLYIM*

Sox6 KO#2 (16nt del) MSSKQATSPFACAADGEETMTQDLERATVISTRPLICLYIM* Fnip1 wild-type
TGTGTATCAGGACTGTGAGAGAAGAGGACGGAATGTCTTGTT

Fnip1 KO#3: 5nt del/1nt in
TGTGTATCAGGACTGTGAGAG----GACGGAATGTCTTGTT
TGTGTATCAGGACTGTGAGAGGACGGAATGTCTTGTT
TGTGTATCAGGACTGTGAGAGGAGGACGGAATGTCTTGTT
Tnt in

Fnip1 wild-type (exon1/2)
MPPTLFQKLFNKKHGLTSPARDARDDCVFSWPLPEFDPSQIRLIVYQDCERRGRNVLF
DSSAKRKIEDVSVS

Fnip1 KO#3 (5nt del)
MPPTLFQKLFNKKHGLTSPARDARDDCVFSWPLPEFDPSQIRLIVYQDCERTECLV*

Fnip1 KO#3 (1nt in)
MPPTLFQKLFNKKHGLTSPARDARDDCVFSWPLPEFDPSQIRLIVYQDCERRRTECLV*

Figure 2.

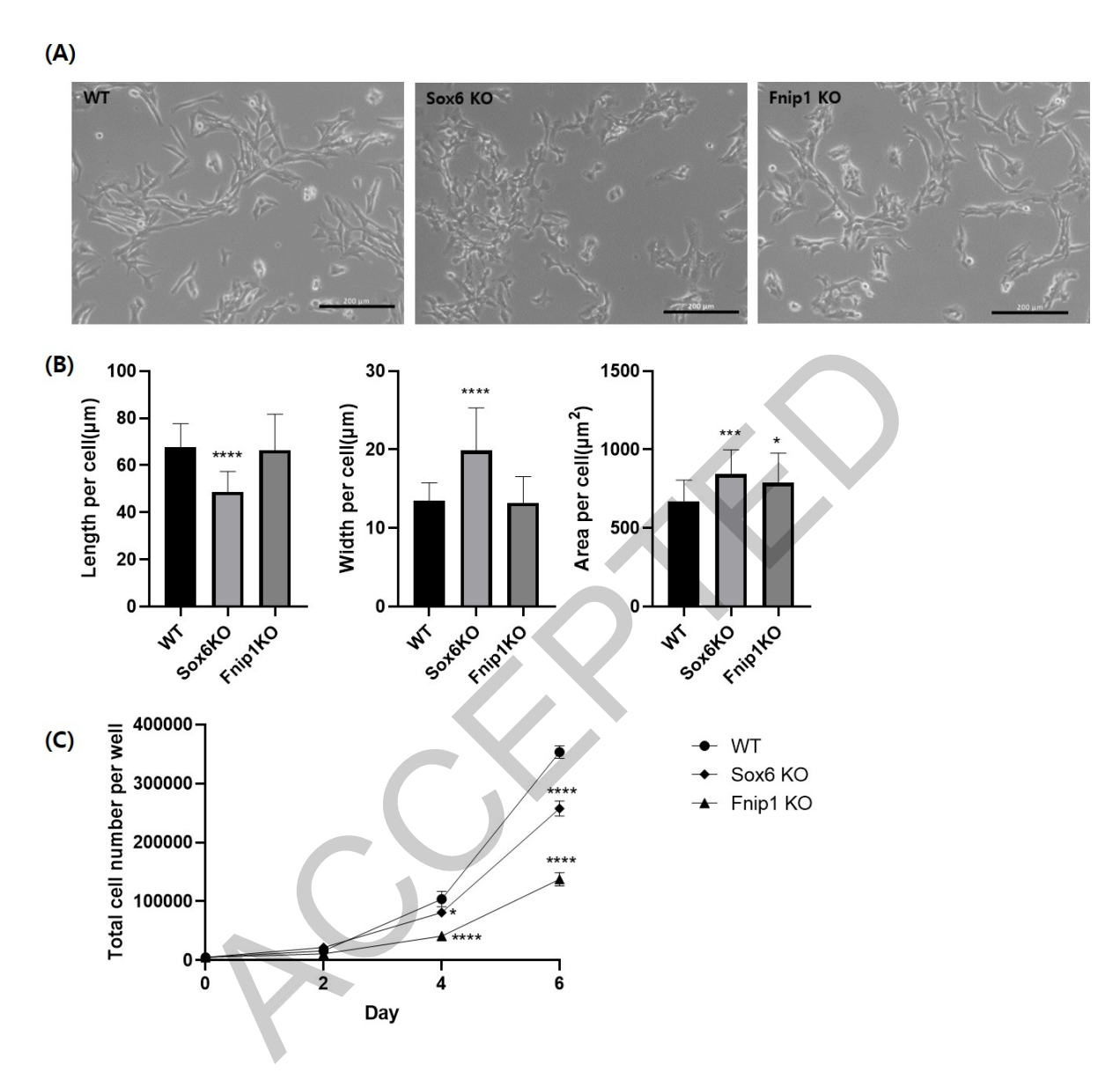


Figure 3.

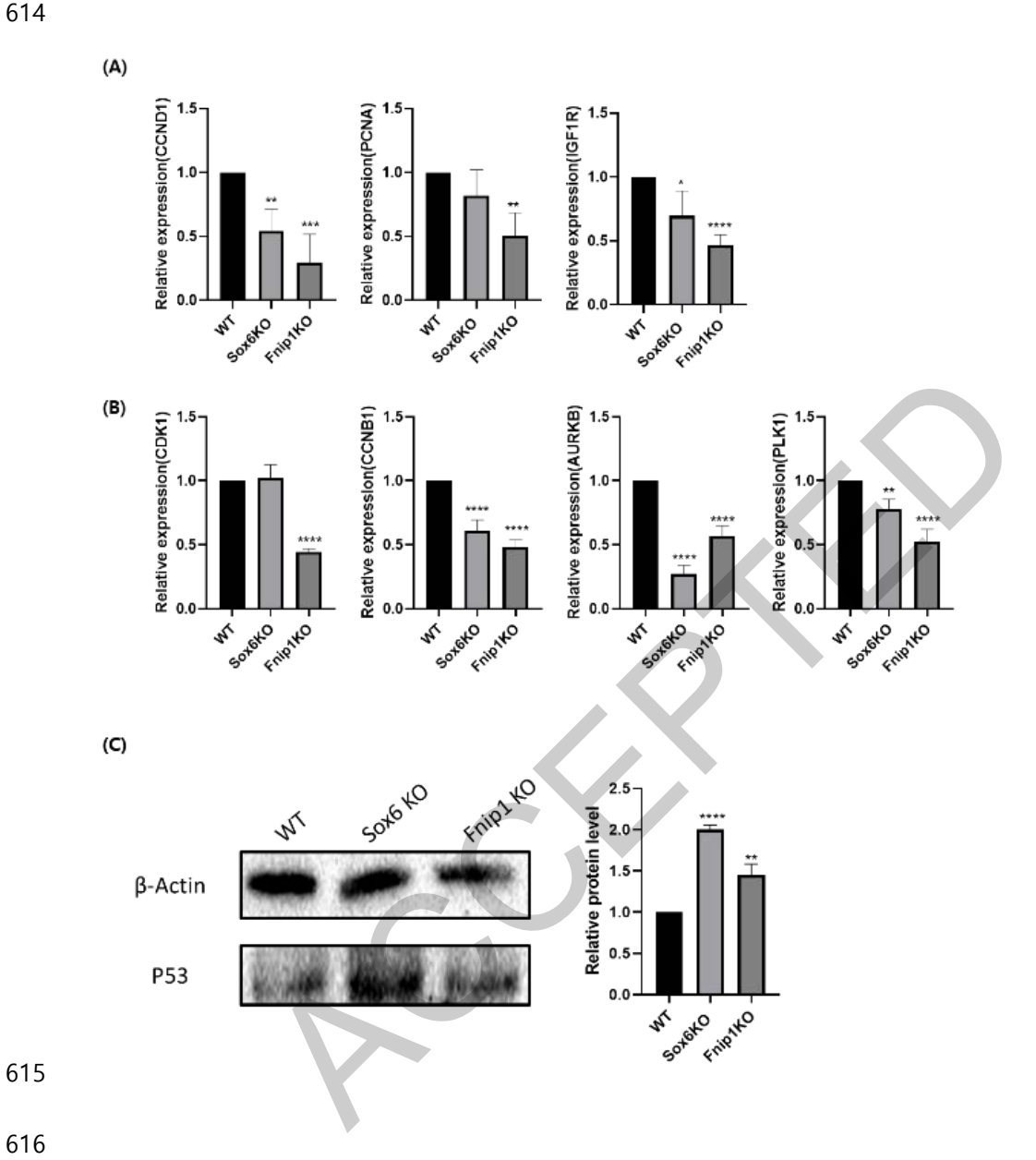
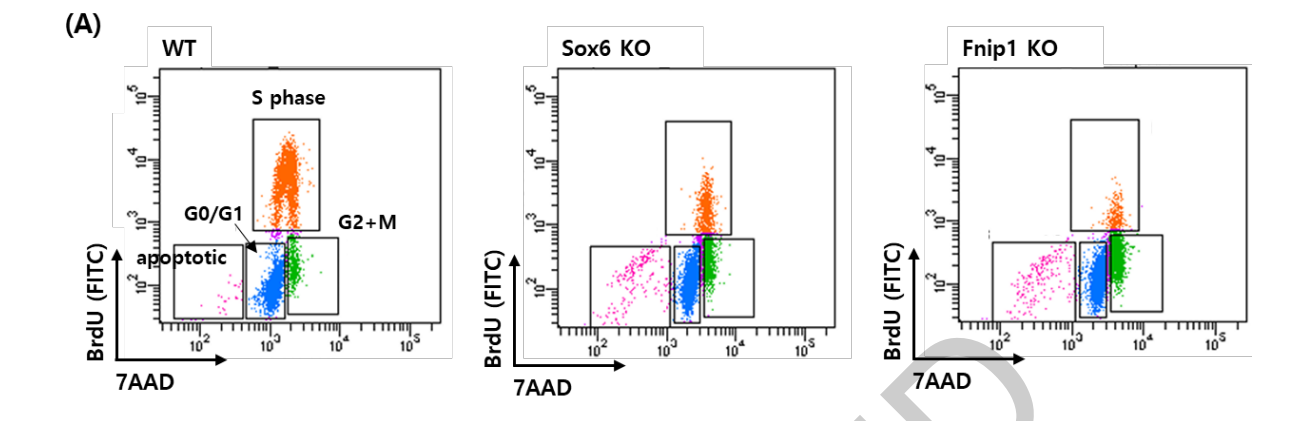


Figure 4.



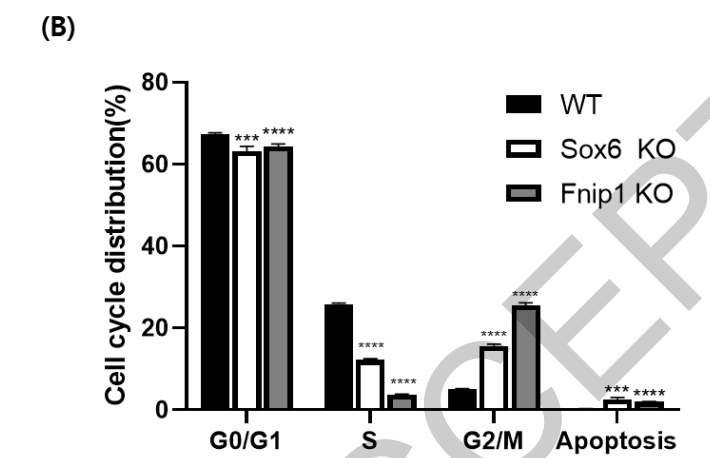


Figure 5.

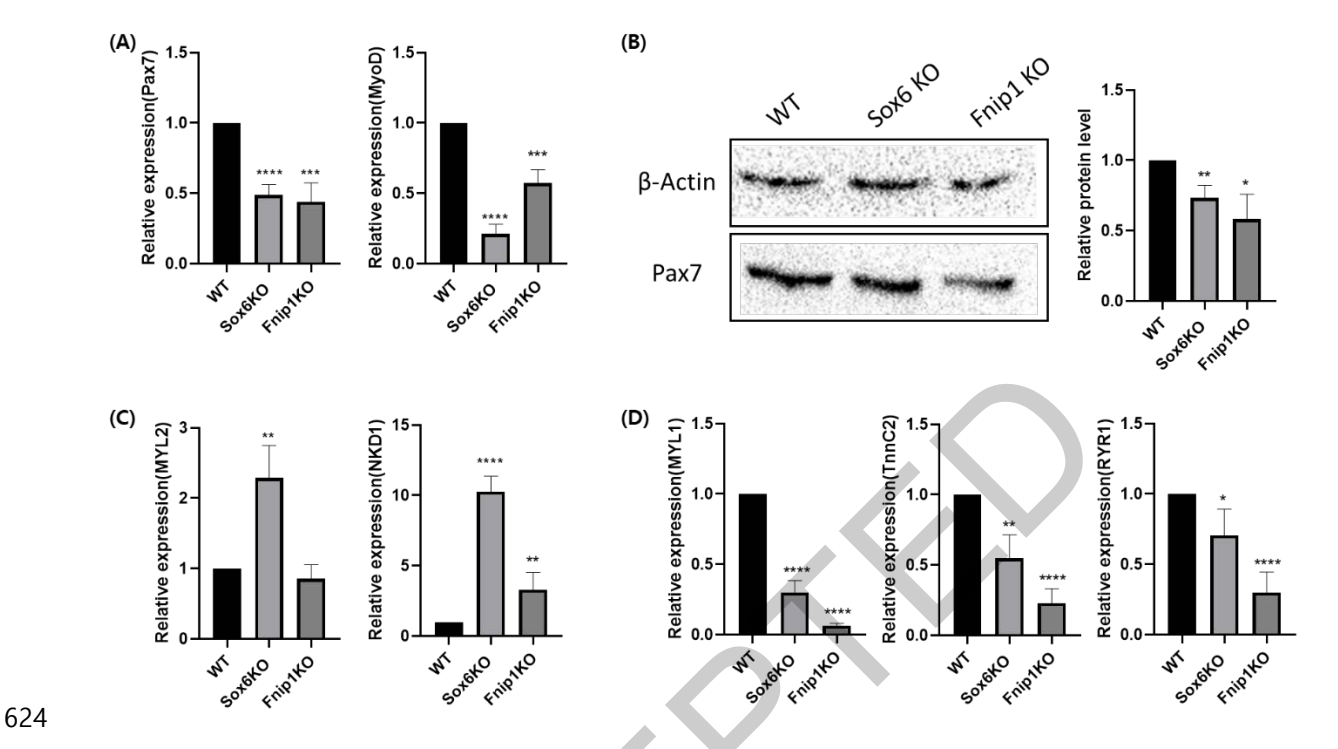


Figure 6.



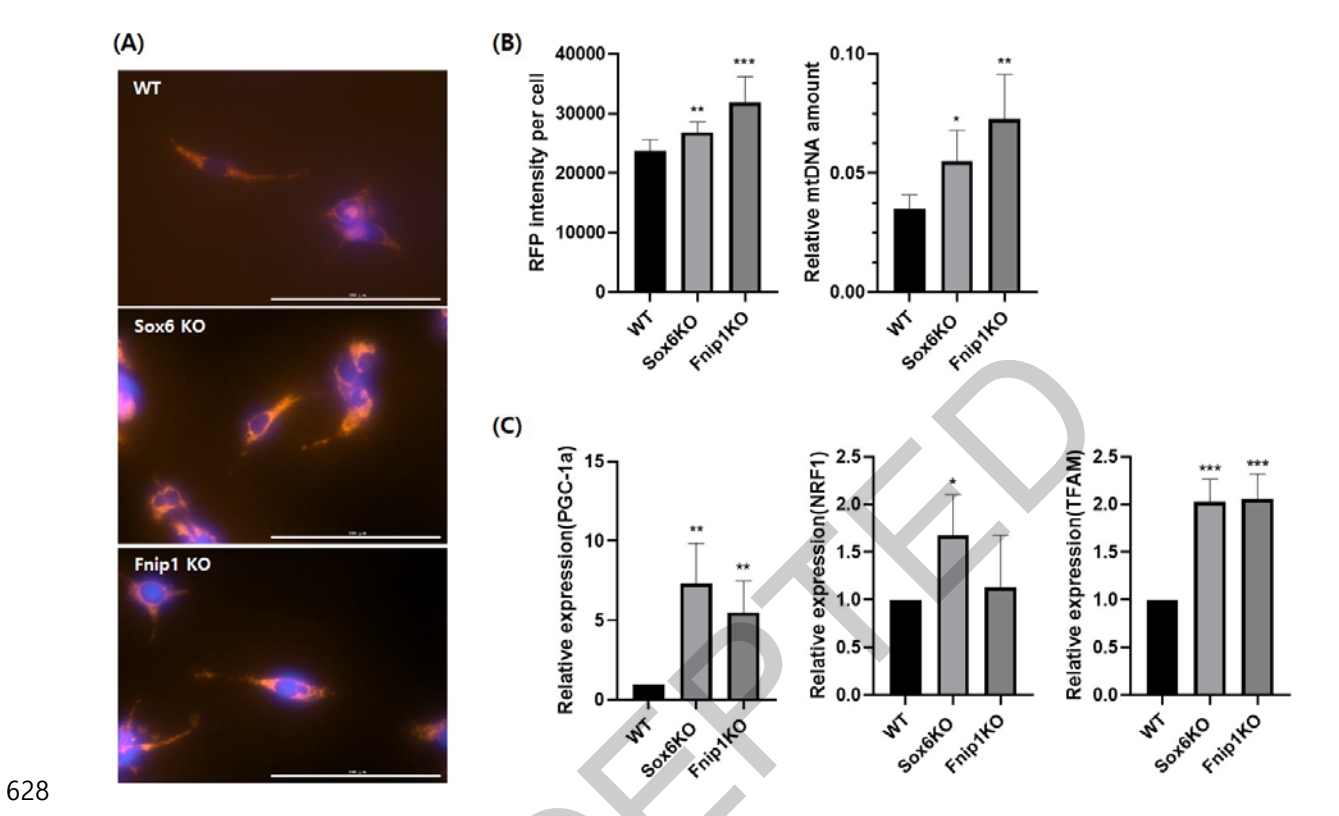


Figure 7.

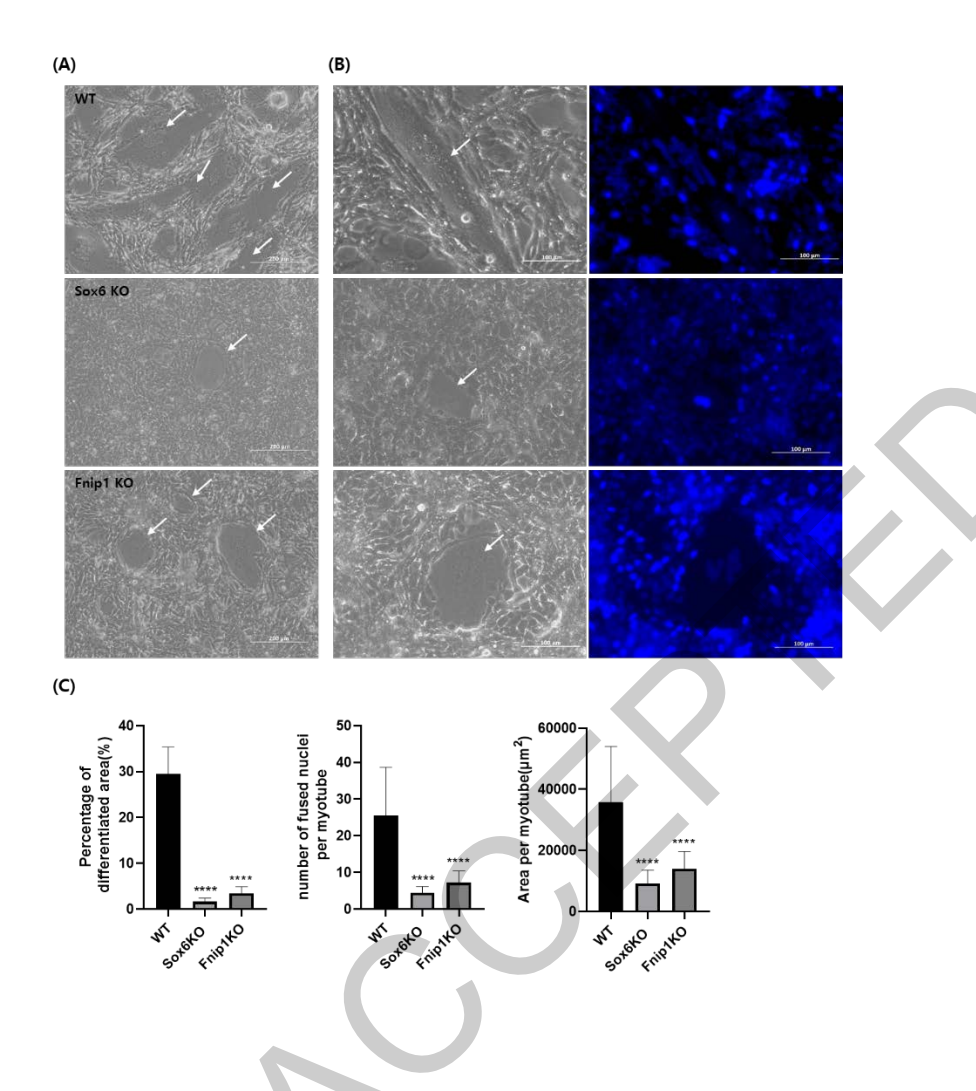


Figure 8.

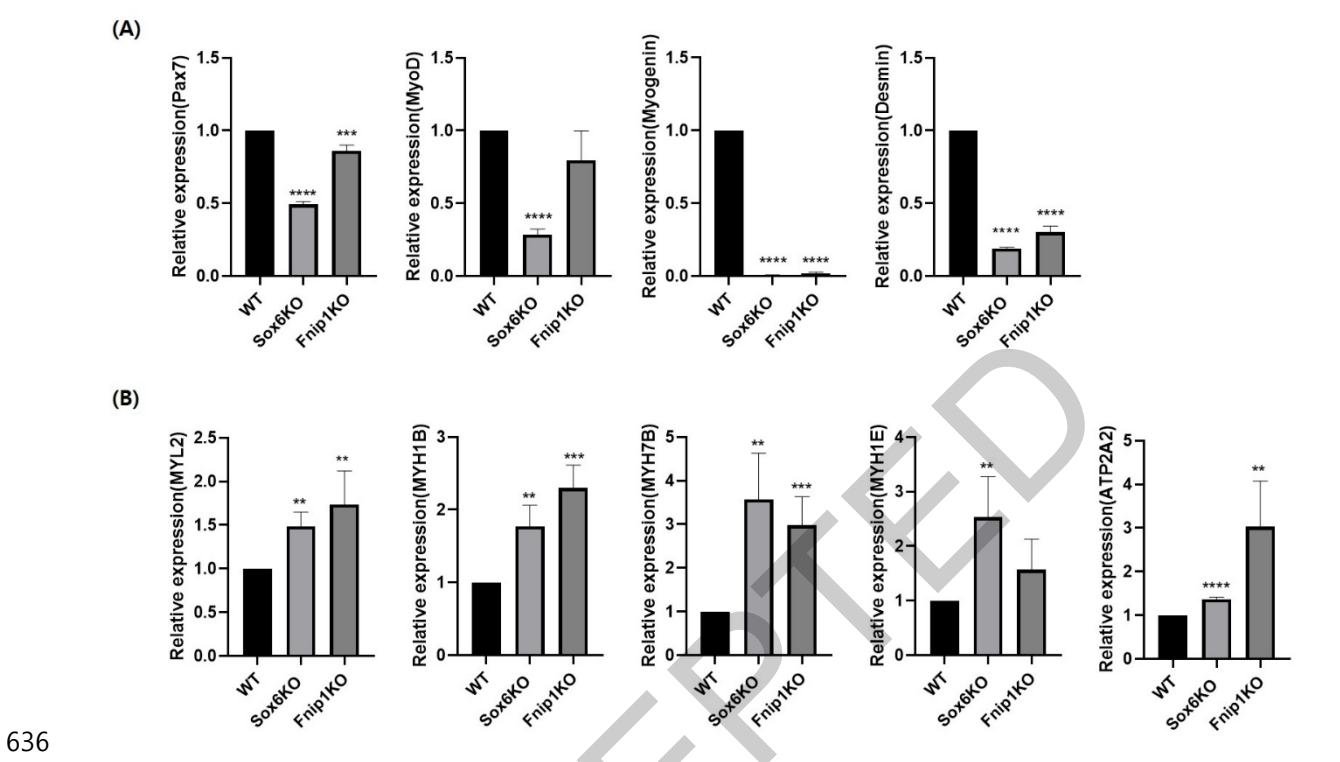


Figure 9.

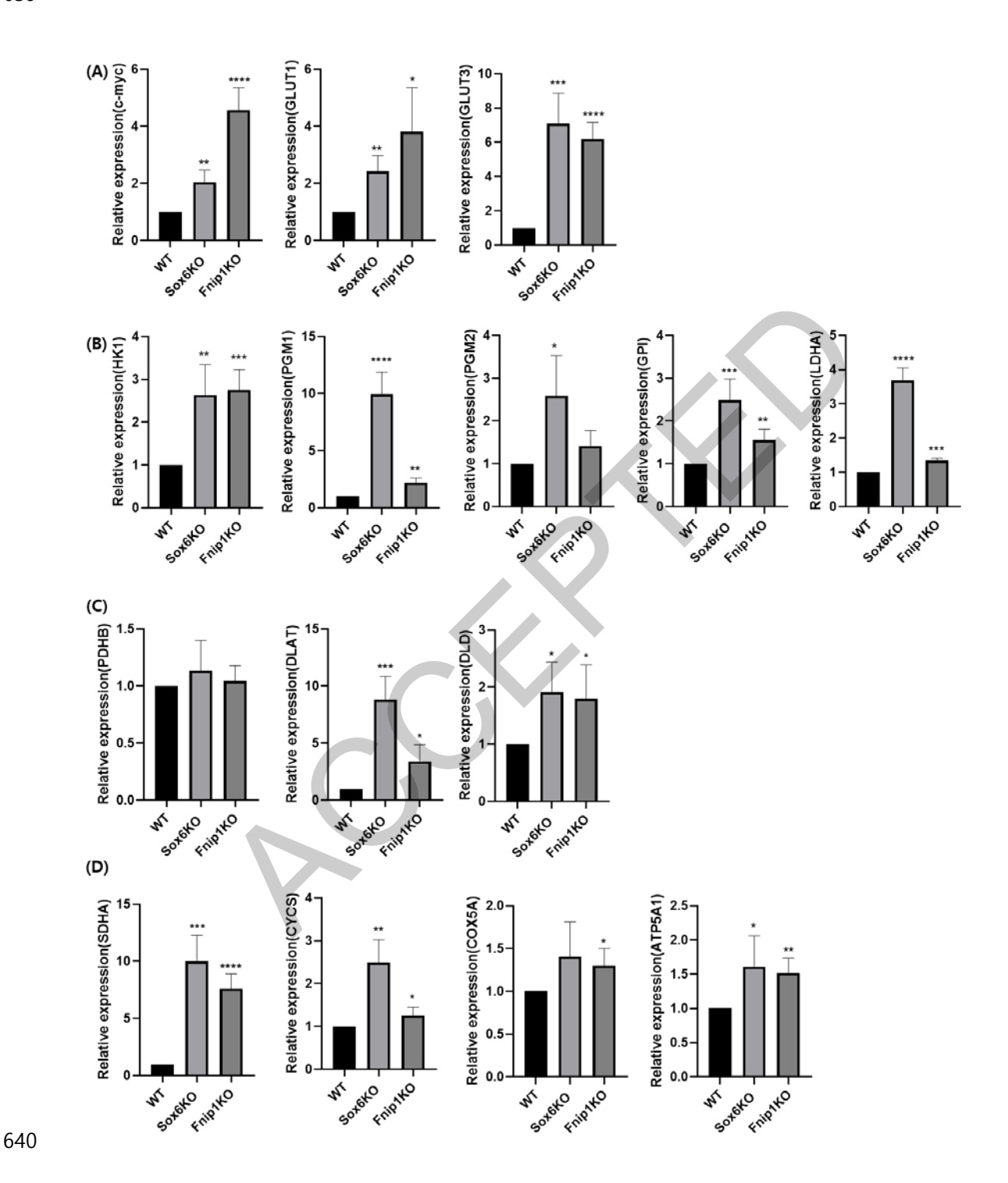
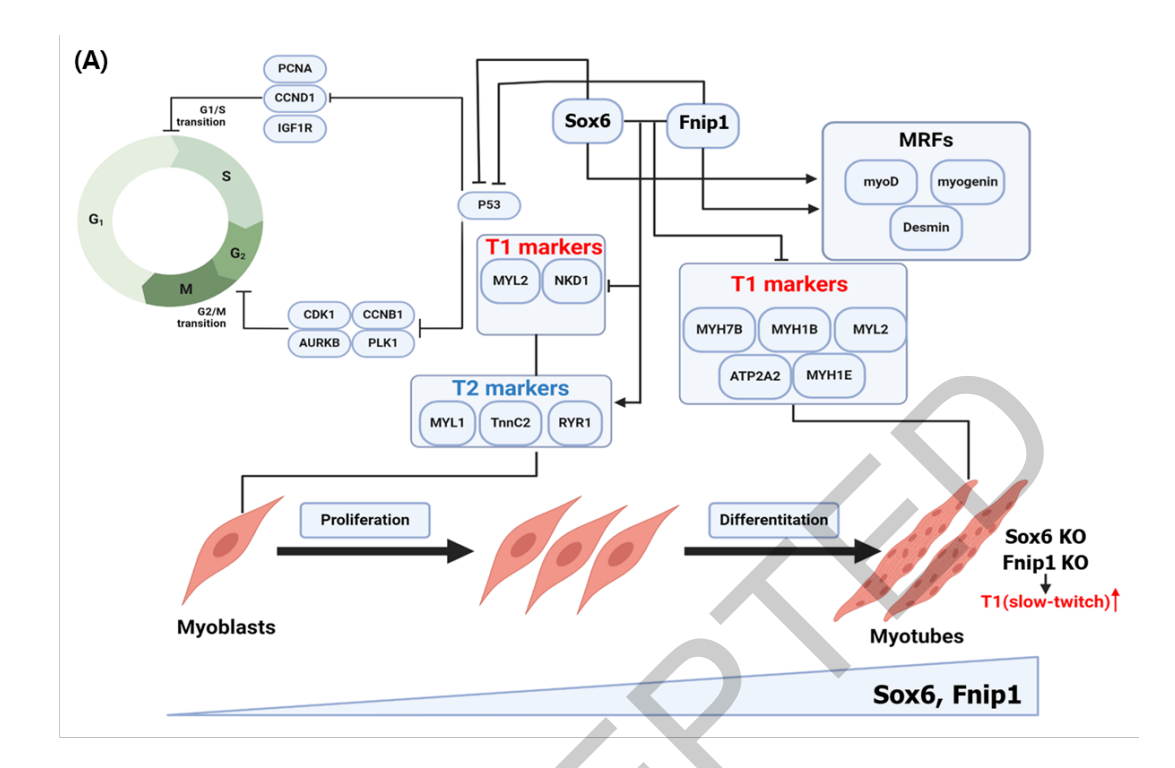
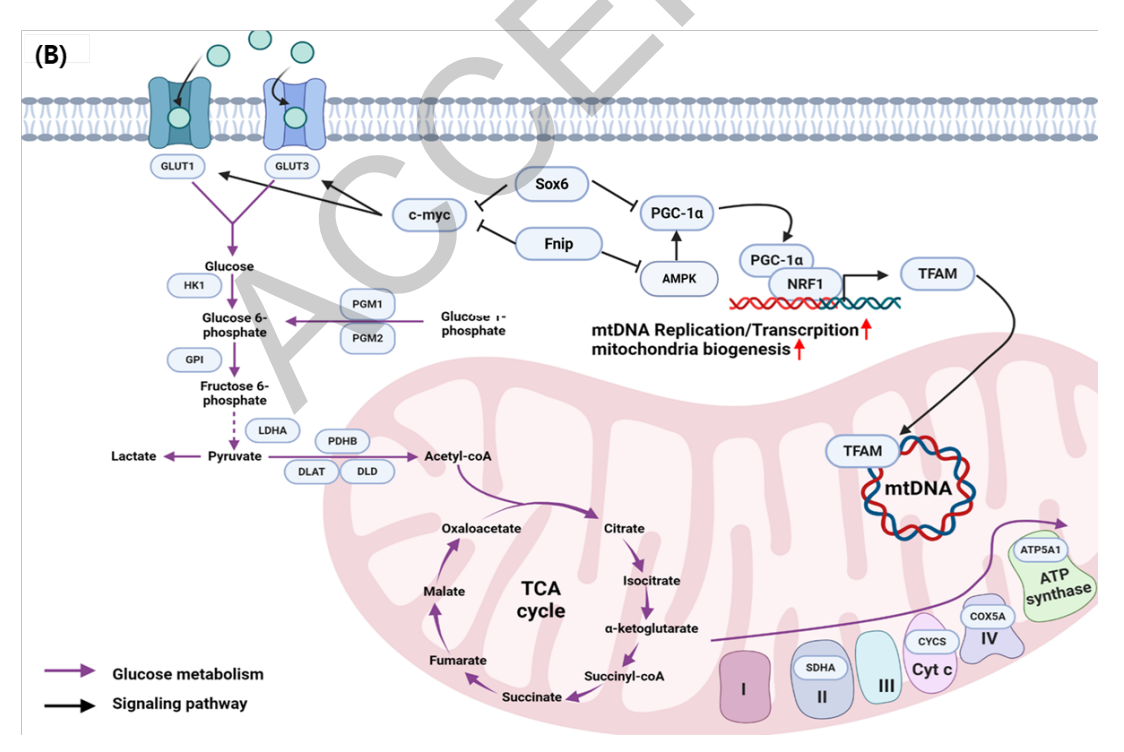


Figure 10.





target gene sequences		annealing
F: 5'-CACGACCATCCAACAAGATG-3'		
R: 5'-TCAGCTGGGTGATCATGGTA-3'	419bp	60°C
F: 5'-CCCTGGGTGACAGTGAAAGT-3'		
R: 5'-CCAGGTGCATGACACAAAAG-3'	498bp	60°C
	411bp	60°C
	·····	
	433bp	60°C
	.ссср	
	195hn	60°C
	1750р	00 0
	553hn	60°C
	3330p	00 C
	410hn	60°C
	4180p	00 C
	1001	60°C
	429bp	60°C
	5001	60°G
	539bp	60°C
	593bp	60°C
	417bp	60°C
R: 5'-TGTGTCCCATCCCAAGGGTA-3'	347bp	60°C
F: 5'-GAGCTGCTTGGGTCCATGAC-3'		
R: 5'-TCAGTGCTTGGGTCCATGAC-3'	345bp	60°C
	374bp	60°C
	2601	60°C
	Soupp	60°C
	278hn	60°C
	2100p	00 C
	355bn	60°C
	сссор	00 0
R: 5'-GATGAACCCATCAGCGTTCT-3'	302bp	60°C
F: 5'-CCAAGAGCTGTCACATCGAA-3'	•	
R: 5'-TCCAACATCTTCTGCTGCAC-3'	274bp	60°C
F: 5'-AGCCTCAACCAGCAGGAGC-3'		
	279bp	60°C
	22.41	5000
	334bp	60°C
	0751	60°C
	213bp	60°C
	160hn	58°C
F:5'-AGACGGCTTCATCGACAAGG-3'	1070p	36 C
R:5'-TGTGTGATGACGTGGACGAG-3'	360bp	60°C
	F: 5'-CACGACCATCCAACAAGATG-3' R: 5'-TCAGCTGGGTGATCATGGTA-3' F: 5'-CCCTGGGTGACAGTGAAAGT-3' R: 5'-CCAGGTGCATGACACAAAAG-3' F: 5'-AGGTACCAAGAGAGCGGCTC-3' R: 5'-CTCGGCAGTGAAAGTGGTCC-3' R: 5'-ACACGTCGGACATGCACTTC-3' R: 5'-ACACGTCGGACATGCACTTC-3' R: 5'-TCTGACTCCCCGCTGTAGTG-3' F: 5'-AATAGTCGCCACTTGGATGC-3' R: 5'-TTTTCTGCGGTCAGAGGAAT-3' F: 5'-GCTCTGAGGGCTTCGACAC-3' R: 5'-TGCTTGAGGGCTTCGACAC-3' R: 5'-TGCTTGCAGAGGAACATCTGCA-3' F: 5'-GCTAGAGTTCAGGCCACGTC-3' R: 5'-TGCTTGCAGACTCATTGACC-3' F: 5'-CCTTTCCATGGACCTCAAGA-3' R: 5'-TTGTTGGGTGTCCCTAAAGC-3' F: 5'-CGACGTTCTTGGCCATATGC-3' F: 5'-CAATCAGACAACGCAGCAGC-3' R: 5'-TTTCTGGCTTGATGTCCCGG-3' R: 5'-TTTCTGGCTTGATGTCCCGG-3' R: 5'-TGGGAGCGATTGAAACCGA-3' F: 5'-GATTCTTCACCTGGGTGGCA-3' R: 5'-TGGTGCCATCCAAGGGTA-3' F: 5'-GAGCTGCTTGGCCATGAC-3' R: 5'-TGGTCCCATCCCAAGGGTA-3' F: 5'-GAGCTGCTTGGGTCCATGAC-3' R: 5'-TGGTCCCATCCCAAGGGTA-3' F: 5'-GAGCTGCTTGGCTCATGAC-3' R: 5'-TCAGTGCTTGGGTCCATGAC-3' R: 5'-TCAGTGCTTGGGTCCATGAC-3' R: 5'-TCAGTGCTTGGGTCCATGAC-3' R: 5'-TCAGTGCTTGGGTCCATGAC-3' R: 5'-TCAGTGCTTGGGTCCATGAC-3' R: 5'-TCAGTGCTTGGGTCCATGAC-3' R: 5'-TCAGTGCTTGGTTCATGACAGC-3' R: 5'-TGGGACGAAAACGAAGATC-3' R: 5'-TGTGTGCCCTCTTATGCTT-3' F: 5'-GATCCAAGCAACCT-3' R: 5'-TTTGCCCTTCTCTTATGCTT-3' F: 5'-GATCCAACGAGGAGAGATC-3' R: 5'-TTTGCCCTTCTGCTTATGCTT-3' F: 5'-GATCCAACCAACCT-3' R: 5'-TTGGCCAGCTTCACCAACCT-3' R: 5'-TTGGCCAGCTTCACCAACCT-3' R: 5'-TTGGCCAGCTTCACCAACCT-3' R: 5'-TTGGCCAGCTCACACCT-3' R: 5'-TTGGCCAGCTTCACCAACCT-3' R: 5'-TTGGCCAGCTTCACCAACCT-3' R: 5'-TTGGCCAGCTCAGCGTTC-3' R: 5'-TCCAACATCTTCTGCTGACC-3' R: 5'-TCCAACATCAACCAGCAGAGACCAACCA-3' R: 5'-TCCAACAGCAGGAGAGAGACAACCA-3' R: 5'-TCCAACAGCAGGAGAGAGAGAGAGAGAGAGAGAGAGAGAG	F: 5'-CACGACCATCCAACAAGATG-3' R: 5'-TCAGCTGGGTGATCATGGTA-3' R: 5'-CCCTGGGTGACAGTGAAAGT-3' F: 5'-CCCTGGGTGACAGTGAAAGT-3' R: 5'-CCCTGGGTGACAGTGAAAGT-3' R: 5'-CCAGGTGCATGACACAAAAG-3' R: 5'-CCAGGTGCATGACACAAAAG-3' R: 5'-CTCGGCAGTGAAAGTGGTCC-3' R: 5'-CTCGGCAGTGAAAGTGGTCC-3' R: 5'-TCTGACTCCCCGCTGTAGTG-3' R: 5'-TCTGACTCCCCGCTGTAGTG-3' R: 5'-TTTTCTGCGGTCAGAGGAAT-3' R: 5'-TTTTCTGCGGTCAGAGGAAT-3' R: 5'-ACAACGAGAGGACATCTGCA-3' R: 5'-ACAACGAGAGGAACACTTGCA-3' R: 5'-ACAACGAGAGGAACATCTGCA-3' R: 5'-TGCTTGCAGACTCCATGACC-3' R: 5'-TGCTTGCAGACTCATTGACC-3' R: 5'-TGTTGCAGACTCCAAAGC-3' R: 5'-TTGTTGGGTGCCATTGACC-3' R: 5'-TGTTGCAGACTCCAAAGC-3' R: 5'-TGTTGCAGACTCCAAAGC-3' R: 5'-TGTTGCAGACTCCAAAGC-3' R: 5'-CAATCAGACAACGCAGCAGC-3' R: 5'-TTTTCTGGCTTGATGTCCCGG-3' R: 5'-TGGTGCCAGTCATTGACC-3' R: 5'-TGGTGCCATTGACC-3' R: 5'-TGGTGCCATTGACC-3' R: 5'-TGGGAGCATTGAAAACCGA-3' R: 5'-TGGTGCCATTGGCCTG-3' R: 5'-TGGTGCCATTGGCCAGCAGC-3' R: 5'-TGGTGCCATTCCCAAAGGCAGC-3' R: 5'-TGGTGCCATTCCCAAGGGTA-3' R: 5'-TGGTCCCATCCCAAAGGCAGC-3' R: 5'-TGGTGCCATTGGCCTG-3' R: 5'-TGGTCCCATCCCAAAGGGTA-3' R: 5'-TGGTCCCATCCCAAAGGGTA-3' R: 5'-TGGTCCCATCCCAAAGGGTA-3' R: 5'-TGGTCCCATCCCAAAGGGTA-3' R: 5'-TGGTCCCATCCCAAAGGGTA-3' R: 5'-TGGTGCCATTGGCCTTGATGCCT3' R: 5'-TGGTCCCATCCCAAGGGTA-3' R: 5'-TGGTGCAAAACGAAGATCC-3' R: 5'-TGGTGCATGACCAGCAGCAGC-3' R: 5'-TGGTGCAAAACGAAGATCC-3' R: 5'-TGGTGCATGACCATCAACCT-3' R: 5'-TGGTGATGACCATCAACCT-3' R: 5'-TGGTGATGACCATCAACCT-3' R: 5'-TGGTGATGACCATCAACCT-3' R: 5'-TGGTGAGAGACCAATCAACCT-3' R: 5'-TGGTGAGAGACCAATCAACCT-3' R: 5'-TCCAAGAGCATCAACCT-3' R: 5'-TCCAAGAGCATCAACCT-3' R: 5'-TCCAAGAGCATCAACCT-3' R: 5'-TCCAAGAGAGAGATCC-3' R: 5'-TCCAAGAGACCAATCAACCT-3' R: 5'-TCCAAGAGCCACATCAACCT-3' R: 5'-TCCAAGAGCCTTCATCCAAGCAGAGAGAGTC-3' R: 5'-TCCAAGAGCAACATCAACCT-3' R: 5'-TCCAAGAGCCTGGAGAGAGAGAGAGAGGTC-3' R: 5'-TCCAAGAGACCAACAGGAGAGAGAGAGAGAGAGAGAGAGA

(NM_001271973.2)	R:5'-TGGCTCAGCTGGTAAAAGGT-3'	370bp	60°C
MYH1E	F: 5'-GGAGACCTGAACGAAATGGA-3'		
(NM_001397409.1)	R: 5'-TCTGCATGTGGAGAAGTTGC-3'	301bp	55°C
C-MYC	F: 5'-GGAGAACGACAAGAGGCGAA-3'		
(KU981087.1)	R: 5'-GTTCTCTCCTCCGCCTCAAC-3'	224bp	60°C
GLUT1	F: 5'-ACAACAGATGTCAGCAGCGA-3'		
(NM_205209.2)	R: 5'-ATCCAGGGCATTTGGTCCAG-3'	392bp	60°C
GLUT3	F: 5'-TTCTTCAAAAGCTCCGTGGT-3'	-	
(NM_205511)	R: 5'-TCTTCAGAGCCAAAGCAAT-3'	397bp	60°C
HK1	F: 5'-AGTCTGGACGCTGGTATCCT-3'		
(NM_204101.2)	R:5'-CCTTGCTCACCATCCACCAT-3'	275bp	60°C
PGM1	F: 5'-CATCCAGATCATCGTCCGCA-3'		
(NM_001038693.3)	R: 5'-CAATGGTACCCAGGTCCACC-3'	302bp	60°C
PGM2	F: 5'-ATATGTGCTGCCCTGCTGTT-3'		
(NM_001031383.2)	R: 5'-CATTGTGGCCACTCCTCCAT-3'	386bp	60°C
GPI	F: 5'-CCAGCAGGGTGACATGGAAT-3'		
(NM_001006128.2)	R: 5'-CAAGGCCTCAGTCTGAGCAA-3'	253bp	60°C
LDHA	F: 5'-CATGGCAGCCTCTTCCTCAA-3'		
(XM_046917898.1)	R: 5'-GAGTCCAGATTGCAGCCACT-3'	302bp	60°C
DLD	F: 5'-GTGTTGAAGGGATGGCTGGA-3'		
(NM_001030727.3)	R: 5'-CTTTGCCAAAAGACGCTGCT-3'	399bp	60°C
PDHB	F: 5'-AAGCGATCGACCAGGTCATC-3'		
(NM_001198620.2)	R: 5'-AGGCCTAGAGTGTGCCACTA-3'	383bp	60°C
DLAT	F: 5'-TCAGCAACATTCGGAGGGTC-3'		
(XM_417933.8)	R: 5'-ACCTTCTCGGGCTTTAGCTG-3'	380bp	60°C
SDHA	F: 5'-AAGGATGTCGTGGAGAGGGA-3'		
(NM_001277398.1)	R: 5'-CACGACCAAAGACCACCAGA-3'	471bp	60°C
CYCS	F: 5'-CCCAGTGCCATACGGTTGAA-3'		
(NM_001398298.1)	R: 5'-GCATCTGTGTAAGAGAAGCCCT-3'	109bp	60°C
COX5A	F: 5'-GGGTCACAGGAGTCAGATGAAG-3'		
(XM_040680176.2)	R: 5'-CCTCTGGAGTGGAGATTCCTAGT-3'	301bp	60°C
ATP5A1	F: 5'-TGTTGTGAAGAGGACCGGTG-3'		
(AF332870.1)	R: 5'-GAAGGGGTGCAGCATCAGAT-3'	470bp	60°C
ACTB	F: 5'-AGAAAATCTGGCACCACACC-3'		
(NM 001101)	R: 5'-CTCCTTAATGTCACGCACGA-3'	395bp	60°C

Supplementary Table 2. The antibody list for Western blotting

Antibody	Company	Dilution ratio	Cat #	Host
β-actin	Santa Cruz	1:1000	sc-47778	Mouse
Pax7	R&D systems	1:500	MAB1675	Mouse
P53	St John's Lab	1:500	STJ140114	Goat
Goat anti-Mouse	Bio-Rad	1:1000	170-6516	Goat
Rabbit anti-Goat	Bio-Rad	1:1000	172-1034	Rabbit

Supplementary Table 3. Primer list for quantification of mitochondria DNA

target gene	sequences	size	annealing
VIM	F: 5'-GCAGATGCAGTAGGCATTCA-3'		
(nucDNA)	R: 5'-GCTGCACTTAGGGCACAAAT-3'	154bp	60°C
D-loop	F: 5'-ACCCCTGCCTGTAATGTACTT-3'		
(mtDNA)	R: 5'-CACGGACTAAAGAGGGGAAGA-3'	183bp	60°C



652 **Supplementary Figure 1.**

(A)

Gallus gallus Sox6 (exon1)

cttcatcta gtggtttgga tttggttccc caaacctgtg cttttatgag tactttcctt gactgtgtat gattaatttt atttgatgta ggcaagtgta ccttctatac cttctatctg gtgtgtatag aggactgttt gagtttgatt tttttgttg acacaaatgt tttctttttg tctccttatt ttgcagaaga ATGTCTTCCA AGCAGGCTAC CTCTCCATTT GCATGTGCAG CTGATGGAGAG GGAAACAATG ACCAGGACT TAGCATCACG AGACAAGGAA GAGGGCAACA GTGATCAGCA CGGACCTCT CATCTGCCTC TACATAATGT AATGCACAAC AAACCTCACT CTGAGGAGCT ACCAACTCTA GTCACGACCA TCCAACAAGA

Gallus gallus Fnip1 (exon2)

agggtttgat gaaatgacat tgcatttgtt ggatttctg ctttaataag gttggctata gagataatgc agaaagaaca gtgcattaaa gagctgtggt aattgatcct tctggtgttc tgtgttttaa ttaaagCTGG CCTTTGCCGG AGTTCGACCC AAGTCAGATC CGACTGATTG TGTATCAGGA CTGTGAGAGA AGAGAGGA AGTTCTGTT TGACTCCAGT GCTAAAAGGA AAATAGAGGA TGTTTCTGTG TCGgtgagta ttgtgcctat gcctgtattc tatattttc aacgtaagat tgataaagta taaaagttct gctttagcca tattaacatt taaactttgg ttacatgcag agctatattt aaaagctgca aattattcag gcttcagtga tttcactctt agcagtttta agtgccatgg tgatctcttt



lac promoter LacZa U6 promoter Fnip1 gRNA LacZa Amp' pUC ori

ECON III GIACOMMANGE AGECT TITAM GOUNCE MITTENET GENET GAT TE CORP. INC. MORE TE GEGEN AGANGAGE CE TIT TIT CECT GITT III GIACOMMAN AGECT GAT AGANGA MAGA TA TIAG TA CAMATA CECT GATAT TE CATATA TE CATATA TA CAGATA CAGATA TA CAGA

Supplementary Figure 2.



